Received: 10 September 2019 | Revised: 10 December 2019 | Accepted: 2 January 2020

DOI: 10.1002/mgg3.1126

ORIGINAL ARTICLE

Molecular Genetics & Genomic Medicine Open Access WILEY

Common and distinct features of potentially predictive biomarkers in small cell lung carcinoma and large cell neuroendocrine carcinoma of the lung by systematic and integrated analysis

Shenghua Dong[1] | **Jun Liang**[2] | **Wenxin Zhai**[1] | **Zhuang Yu**[1]

[1]Department of Oncology, The Affiliated Hospital of Qingdao University, Qingdao, Shandong, China

[2]Department of Oncology, Peking University International Hospital, Beijing, China

Correspondence
Zhuang Yu, The Affiliated Hospital of Qingdao University, No. 16 Jiangsu Road, Shinan District, Qingdao 266003, China.
Email: yuzhuang2002@163.com

Funding information
Natural Science Foundation of Shandong Province, Grant number: ZR2017MH062; Science and Technology for People's Livelihood Project of Qingdao, Grant number: 17-3-3-33-nsh.

Abstract

Background: Large-cell neuroendocrine carcinoma of the lung (LCNEC) and small-cell lung carcinoma (SCLC) are neuroendocrine neoplasms. However, the underlying mechanisms of common and distinct genetic characteristics between LCNEC and SCLC are currently unclear. Herein, protein expression profiles and possible interactions with miRNAs were provided by integrated bioinformatics analysis, in order to explore core genes associated with tumorigenesis and prognosis in SCLC and LCNEC.

Methods: GSE1037 gene expression profiles were obtained from the Gene Expression Omnibus (GEO) database. Differentially expressed genes (DEGs) in LCNEC and SCLC, as compared with normal lung tissues, were selected using the GEO2R online analyzer and Venn diagram software. Gene ontology (GO) analysis was performed using Database for Annotation, Visualization and Integrated Discovery. The biological pathway analysis was performed using the FunRich database. Subsequently, a protein–protein interaction (PPI) network of DEGs was generated using Search Tool for the Retrieval of Interacting Genes and displayed via Cytoscape software. The PPI network was analyzed by the Molecular Complex Detection app from Cytoscape, and 16 upregulated hub genes were selected. The Oncomine database was used to detect expression patterns of hub genes for validation. Furthermore, the biological pathways of these 16 hub genes were re-analyzed, and potential interactions between these genes and miRNAs were explored via FunRich.

Results: A total of 384 DEGs were identified. A Venn diagram determined 88 common DEGs. The PPI network was constructed with 48 nodes and 221 protein pairs. Among them, 16 hub genes were extracted, 14 of which were upregulated in SCLC samples, as compared with normal lung specimens, and 10 were correlated with the cell cycle pathway. Furthermore, 57 target miRNAs for 8 hub genes were identified, among which 31 miRNAs were correlated with the progression of carcinoma, drug-resistance, radio-sensitivity, or autophagy in lung cancer.

Shenghua Dong and Jun Liang contributed equally to this work.

Conclusion: This study provided effective biomarkers and novel therapeutic targets for diagnosis and prognosis of SCLC and LCNEC.

KEYWORDS

bioinformatics analysis, biomarker, LCNEC, lung cancer, SCLC

1 | INTRODUCTION

High-grade pulmonary neuroendocrine neoplasms (NENs), small-cell lung cancer (SCLC), and large-cell neuroendocrine carcinoma of the lung (LCNEC) are among the malignancies with the highest mortality rates. Since the revised 2015 World Health Organization classification of lung tumors classified LCNEC as a NEN (Travis, Brambilla, Burke, Marx, & Nicholson, 2015), debates and investigations of the new classification were ceaseless. LCNEC was grouped with NENs due to its similarities with SCLC in terms of morphology, DNA methylation, protein levels, mutational aspects, and transcriptional levels (Aly et al., 2019; Karlsson et al., 2015, 2014; Miyoshi et al., 2017; Rossi et al., 2005; Simbolo et al., 2017), in spite of a certain extent of heterogeneity (Clinical Lung Cancer Genome Project (CLCGP); Network Genomic Medicine (NGM), 2013; Rossi et al., 2005; Simbolo et al., 2017). In addition, despite the differences in histopathological characteristics between SCLC and LCNEC, their clinical characteristics are similar, including a generally poor outcome, greater incidence in men than in women, and advanced stage diagnosis (Asamura et al., 2006; Cerilli, Ritter, Mills, & Wick, 2001; Xu et al., 2019). With regard to treatment, individuals with SCLC and LCNEC may manifest different sensitivities to different types of treatment, owing to gene alterations between SCLC-like LCNEC and NSCLC-like LCNEC (Rekhtman et al., 2016).

Genome-based medicine, which has been used in oncology for >10 years, can rapidly detect differentially expressed genes and provide greater chances of reducing malignancy-related morbidity and mortality (Vogelstein et al., 2013). Therefore, a number of valuable clues obtained from the SCLC regulation and LCNEC development could be investigated from different perspectives using gene chips. However, the understanding of the genetic expression of these two types of NEN is limited. Genetic analysis was therefore conducted to clarify the genomic characteristics of NENs and determine the similarities between SCLC and LCNEC, consequently identifying more potential genetic candidates for treatment.

In this study, GSE1037 expression microarray data were downloaded from the Gene Expression Omnibus (GEO) database. DEGs were analyzed and their interaction patterns in this dataset were revealed through a protein–protein interaction (PPI) network. In addition, possible DEG functions were explored by gene and biological pathway enrichment analysis. The functions of the significant genes involved in major function terms were discussed, and a number of them might be novel candidates for SCLC and LCNEC treatment. The workflow of the present study is depicted in Figure 1 (free images were obtained from Servier Medical Art).

2 | MATERIALS AND METHODS

2.1 | Ethical compliance

This article does not contain any studies with human participants or animals performed by any of the authors, and therefore no ethical compliance is required.

2.2 | Gene expression profile data

Gene expression profiles (GSE1037) were obtained from the GEO database, based on the GPL962 CHUGAI 41K platform. Data including 18 primary normal lung tissues, 8 primary LCNEC tissues, 15 primary small-cell lung carcinoma tissues, and 9 small-cell lung carcinoma cell lines were downloaded. The profiles of differentially expressed genes in SCLC and LCNEC are presented in a volcano plot online http://www.ehbio.com/ImageGP/.

2.3 | Data processing of DEGs

The mRNA expression raw data were analyzed by GEO2R online tools (Davis & Meltzer, 2007). To identify DEGs in SCLC and LCNEC, as compared with normal lung specimens, $|\log FC| > 2$ and adjusted $p < .05$ were used as the threshold. A Venn diagram was drawn to visualize shared genes in SCLC and LCNEC specimens.

2.4 | Functional enrichment analysis of DEGs

Annotation, Visualization and Integrated Discovery (DAVID) (Huang da, Sherman, & Lempicki, 2009a, 2009b),

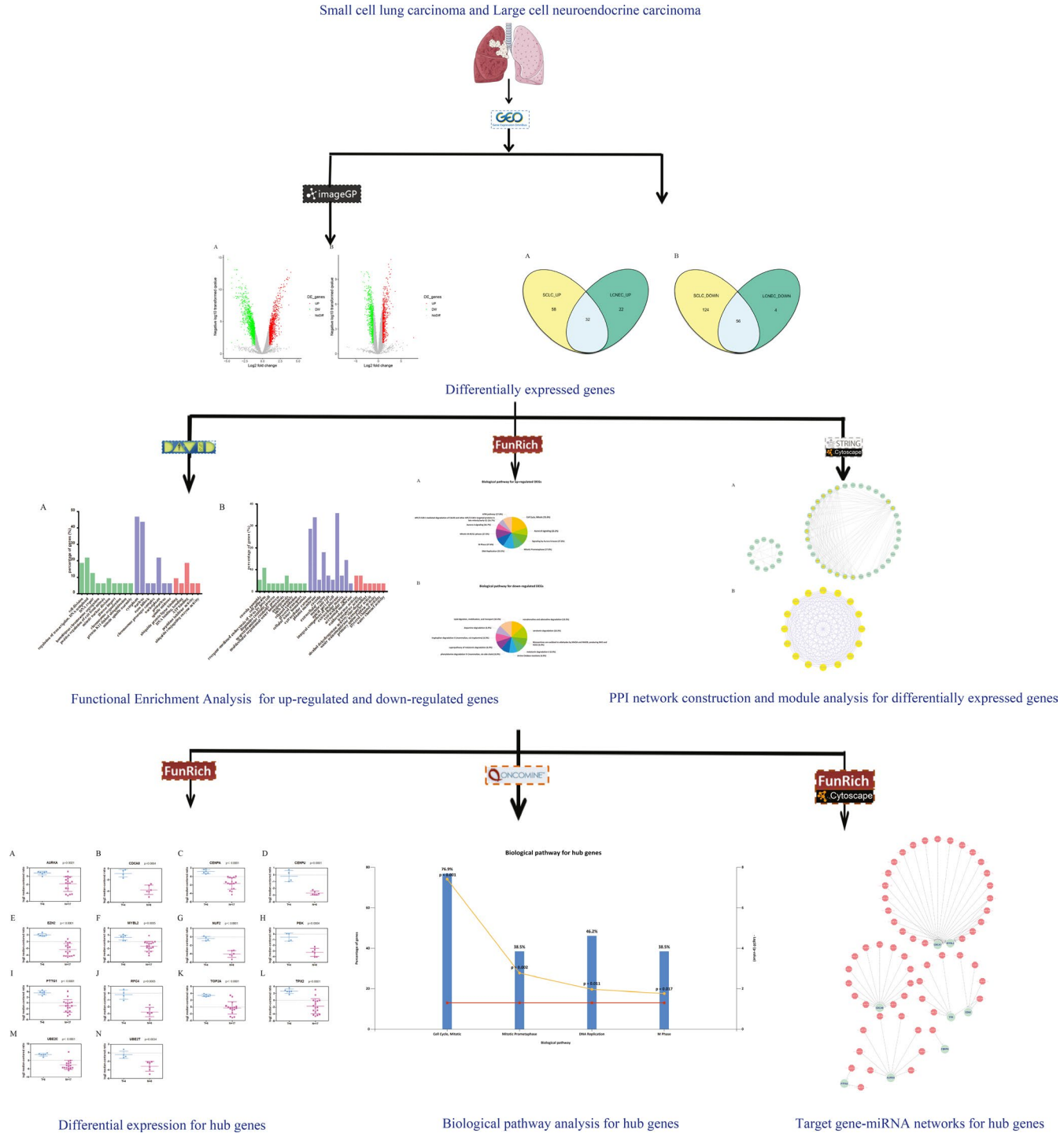

FIGURE 1 Workflow for identification of hub genes and pathways in small cell lung carcinoma and large cell neuroendocrine carcinoma of the lung. Step 1: We identified the differentially expressed genes commonly in small cell lung carcinoma and large cell neuroendocrine carcinoma of the lung. Step 2: The GO and biological pathway analysis were performed and the PPI network was constructed. Next, we identified the hub genes from the PPI network. Step 3: We validated expression patterns and re-analysis biological pathway of hub genes. Then, the target miRNAs associated with hub genes were identified and gene-miRNA networks were constructed. Free images were obtained from Servier Medical Art

a bioinformatics online tool, provides functional annotations and gene analysis. Purpose genes were integrated using Gene ontology (GO) analysis in DAVID, to identify their biological properties. Biological pathway analysis of DEGs and hub genes was performed using FunRich software (Pathan et al., 2017), a self-contained software tool used for function enrichment and interaction network evaluation of sets of genes and proteins.

2.5 | PPI network construction and module analysis

Search Tool for the Retrieval of Interacting Genes (STRING) (Szklarczyk et al., 2015)) is a database of known and potential PPIs. DEGs were evaluated by STRING and a combined score of ≥0.4 was set as the cut-off value. The network was visualized by Cytoscape (Shannon et al., 2003) and the Cytoscape app Molecular Complex Detection (MCODE) was then used to examine marked modules of the PPI network, with the advanced option set to a max. depth of 100, degree cut-off of 2, k-core of 2, and node score cut-off of 0.2.

2.6 | Oncomine analysis

To validate the hub genes, the Oncomine website (www.oncomine.org) was used to obtain mRNA expression data to compare SCLC and normal lung tissues from Bhattacharjee et al. (2001) and Garber et al. (2001).

2.7 | Prediction of target miRNAs for DEGs

To detect predicted miRNAs corresponding to core genes selected from MCODE, miRNA enrichment in FunRich software was performed and miRNAs found to interact with hub genes were defined. The results were input into and visualized by Cytoscape.

2.8 | Statistical analysis

In this study, a student's *t*-test was carried out using GraghPad Prism 5 to generate a *p*-value for the comparison of cancerous specimens and normal control samples. $p < .05$ was considered to indicate a statistically significant difference.

3 | RESULTS

3.1 | Identification of DEGs

DEGs in the SCLC and LCNEC samples, as compared with normal ones, were determined using GEO2R online analyzer (|logFC| > 2 and adjusted $p < .05$) (Davis & Meltzer, 2007). A total of 270 and 114 DEGs were extracted from SCLC and LCNEC samples, respectively. A "volcano plot" between *p*-values and fold changes was established to plot the differentially expressed genes (Figure 2). A Venn diagram was then drawn to confirm the shared DEGs in the two subtypes (Figure 3). Finally, 88 common DEGs were confirmed,

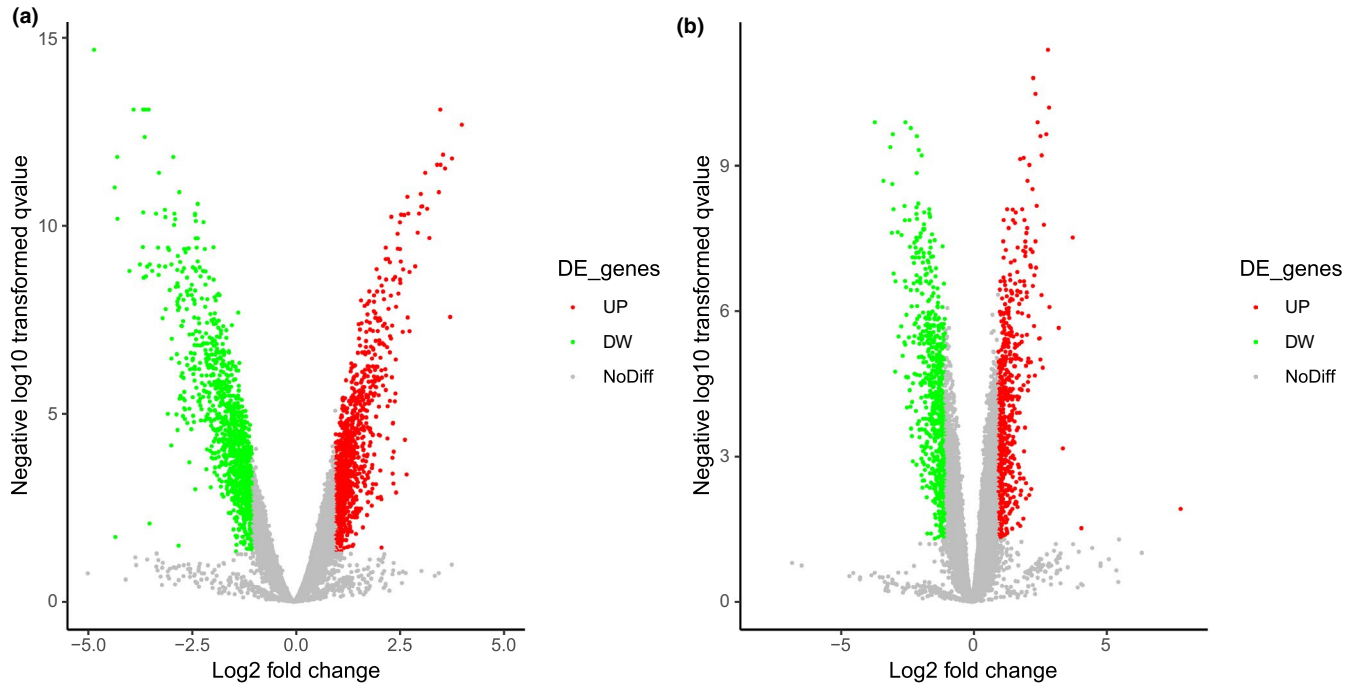

FIGURE 2 Volcano plot of the DEGs. (a) Volcano plot for the DEGs in small cell lung carcinoma, as compared with normal lung samples. (b) Volcano plot for the DEGs in large cell neuroendocrine carcinoma of the lung, as compared with normal lung samples. The x-axis demonstrates the log 2 fold change, and the y-axis demonstrates the log10 (adjusted *p*-value). The red dots indicate up-regulated genes, and the green dots indicate down-regulated genes. The DEGs were filtered on the basis of a |log 2 fold change|> 1.0 and an adjusted *p*-value of < .05. The grey dots represent genes with no significant difference. DEGs, differentially expressed genes

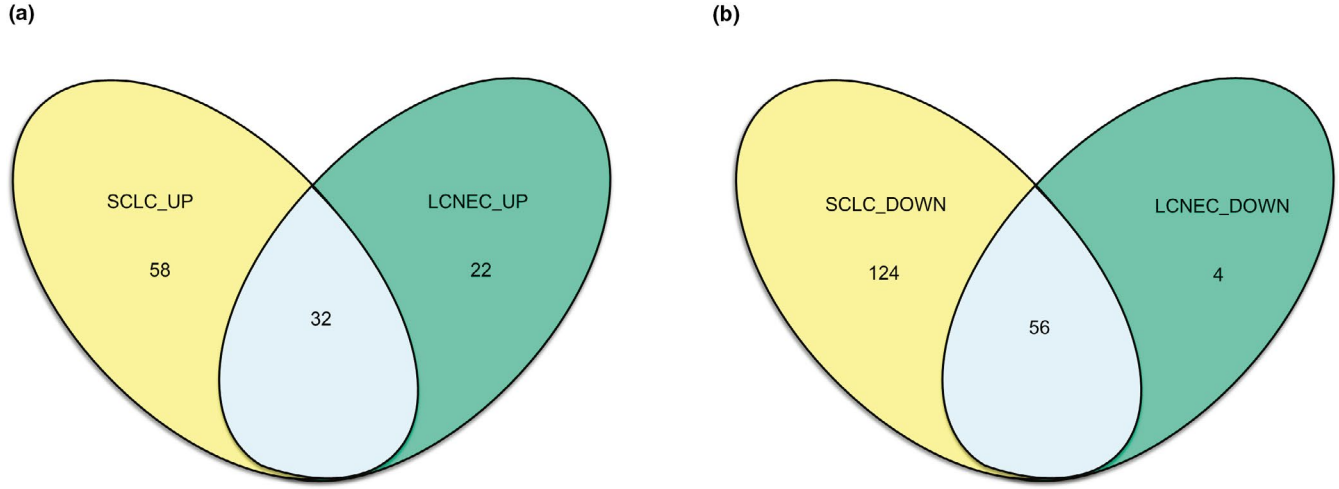

FIGURE 3 Identification of 88 common DEGs in two types of NENs (SCLC and LCNEC) via Venn diagrams. (a) 32 DEGs are upregulated in the two types of NENs (logFC > 0). (b) 56 DEGs are downregulated in the two types of NENs (logFC < 0). Different color meant different types. SClC, small cell lung carcinoma. LCNEC, large cell neuroendocrine carcinoma of the lung

including 56 downregulated and 32 upregulated genes in the SCLC and LCNEC samples (Table 1).

3.2 | Enrichment analysis

All 88 DEGs were analyzed using DAVID and FunRich software. The GO analysis results were as follows: (a) For biological processes (BP), the significantly enriched terms of upregulated DEGs were cell division, regulation of transcription, DNA repair, homologous chromosome segregation, positive regulation of exit from mitosis, mitotic nuclear division, glucose import, chromosome organization, protein K11-linked ubiquitination, mitotic spindle organization and mitotic spindle assembly, and the significant terms of downregulated DEGs were caveola assembly, cell adhesion, receptor-mediated endocytosis of virus by host cell, dopamine catabolic process, neurotransmitter catabolic process, multicellular organismal water homeostasis, angiogenesis, bleb assembly, ethanol oxidation, glycerol transport, and cellular water homeostasis; (b) for molecular function (MF), the notably enriched terms of upregulated DEGs were ubiquitin protein ligase binding, DNA binding, adenosine triphosphate (ATP) binding, peptidase inhibitor activity and ubiquitin conjugating enzyme activity, and those for downregulated DEGs were oxidoreductase, transporter, alcohol dehydrogenase (zinc-dependent), water transmembrane transporter, primary amine oxidase, glycerol channel and water channel activities; (c) for GO cell component (CC), the upregulated DEGs were particularly enriched in cytoplasm, nucleus, axon hillock, chromosome passenger complex, nucleoplasm, pronucleus and spindle midzone, and downregulated DEGs in extracellular exosome, plasma membrane,

TABLE 1 Commonly DEGs in the SCLC and LCNEC samples

DEGs	Genes name
Upregulated	ZNF829 BCCIP PTTG1 CENPA FAM123A SESN2 CSE1L LOC256676///CDCA5 PBK UBE2TC5orf13 ZNF587 UNQ353/// CSNK1G1///KIAA0101 HMGB3 SOX4 FARP1 C1orf215///STMN1 MLF1IP AURKA MYBL2 ZWINTAS///ZWINT UBE2C EZH2 RFC4 CDCA8 SLC2A1 LOC253012 TPX2 TTKCDCA7 TOP2A NUF2
Downregulated	ADH1B CAV1 WIF1 SFTPC FMO2 TSHZ2///ADAMTS8 USP42 MFAP4 SCGB1A1 IGSF10 TIMP3 CLDN18 OGN CAV2 MAOA FABP4 ZNF521 SVEP1 EPAS1 TPSB2///TPSAB1 FHL1 FAT4 CAB39L ADH1C PI4KAP1 C2orf34 AGER LOC144571///PZP///A2M AQP4 FAM75A1 SFTPH AQP1 CAMP HBE1 EMCN HNRNPH1 SLC39A8 SUSD2 FLJ44379 LIMCH1 SLPI CYBRD1 HOPX C13orf15 LOC100131277///TACC1 LYVE1 GPR116 MAOB SELENBP1 PGM5 EMP2 PMP22 S1PR1 ABCA8 ANGPTL1 RGS2

Abbreviations: DEGs, differentially expressed genes; LCNEC, large cell neuroendocrine carcinoma; SCLC, small cell lung carcinoma.

caveola, extracellular region, membrane raft, apical part of cell, integral component of membrane, extracellular matrix, extracellular space, and acrosomal membrane (Table 2). These results are displayed in bar graphs produced on GraghPad Prism 5 (Figure 4).

The biological pathway analysis results are shown in Figure 5, indicating that upregulated DEGs were notably enriched in cell cycle (mitotic), DNA replication, ataxia telangiectasia-mutated (ATM) pathway, mitotic M-M/G1 phases, signaling by Aurora kinases, M phase, mitotic prometaphase, while downregulated DEGs in lipid digestion, mobilization and transport, noradrenaline and adrenaline degradation, and serotonin degradation (Figure 5).

3.3 | PPI network and module analysis

Using STRING, a PPI network containing 48 nodes and 221 protein pairs was constructed, with a combined score of >0.4. As shown in Figure 6, most nodes in the PPI network were upregulated DEGs in SCLC and LCNEC specimens. Next, the MCODE app in Cytoscape was used for further analysis, which showed that 16 of 48 nodes were hub nodes (Figure 6). These core nodes were all upregulated genes: Enhancer of zeste homolog 2 (*EZH2*, OMIM:601573), cell division cycle-associated 1 (*CDCA1/NUF2*, OMIM:611772), PDZ binding kinase, *CDCA8(*OMIM:609977*)*, *CDCA7*(OMIM:609937), aurora kinase A (*AURKA*, OMIM:603072), replication factor C4 (*RFC4*, OMIM:102577), ubiquitin conjugating enzyme E2 C (*UBE2C*, OMIM:605574), centromere protein A (*CENPA*, OMIM:117139), targeting protein for xklp2 (*TPX2*, OMIM:605917), TTK protein kinase (*TTK*, OMIM:604092), V-Myb avian myeloblastosis viral oncogene homolog-like 2 (*MYBL2*, OMIM:601415), pituitary tumor transforming gene 1 (*PTTG1*, OMIM:604147), DNA topoisomerase II α (*TOP2A*, OMIM:126430), centromere protein U (*CENPU*, OMIM:611511), and *UBE2T*(OMIM:610538).

3.4 | Analysis of core genes by the Oncomine database

The Oncomine database (www.oncomine.org) was used to determine the expression patterns of 16 hub genes between normal and cancerous lung tissues. Due to the rarity of LCNEC, the expression pattern was only obtained in SCLC samples and compared with normal lung samples. The results showed that, except for TTK (deficiency in expression data), 14 of 15 genes were highly expressed in SCLC specimens, as compared with normal ones, which was consistent with the GSE1037 data (Figure 7).

3.5 | Re-analysis of hub genes by biological pathway analysis

To better apprehend the pathway correlated with these 16 selected DEGs, biological pathway analysis was performed again by FunRich. The results showed that these 16 core genes were markedly enriched in the cell cycle pathway, mitotic prometaphase, DNA replication and M phase (Figure 8). Among them the cell cycle pathway was the most markedly enriched, containing 10 genes (*CDCA1, CDCA8, AURKA, RFC4, UBE2C, CENPA, CENPU, MYBL2, PTTG1,* and *TOP2A*) ($p = 2.30182e\text{-}11$).

3.6 | Prediction of target miRNAs for hub genes

The target human miRNAs for hub genes were determined by FunRich software, and the mRNA-miRNA network was displayed by Cytoscape (Figure 9). The genes found to be connected with miRNAs were *TTK, PTTG1, MYBL2, EZH2, CENPA, CDCA8, CDCA7,* and *AURKA*. Hub genes and their corresponded target miRNAs are presented in Table 3. Finally, 31 miRNAs, whose functions were correlated with tumor progression (Chang et al., 2019; Chang et al., 2017; Chen et al., 2015; Gao et al., 2018; Gu et al., 2014; Han et al., 2019; He et al., 2019; Kucuksayan et al., 2019; Li, Ma, Zhang, Ji, & Jin, 2014; Li, Ran, et al., 2018; Li & He, 2014; Li, Fu, et al., 2019; Li, Cui, Li, Zhang, & Li, 2018; Liu et al., 2017; Liu, Liu, Deng, et al., 2019; Liu, Liu, & Lu, 2019; Liu, Liu, Zhang, Tong, & Gan, 2019; Liu, Miao, et al., 2016; Luo et al., 2018; Tang et al., 2018; Wang et al., 2017; Wang, Cao, Su, Li, & Yan, 2019; Wu et al., 2015; Wu, Mo, Wan, Dan, & Hu, 2019; Xia, Jing, Li, & Lv, 2018; Xu et al., 2018; Zeng et al., 2018; Zhang, Hao, et al., 2018; Zhang et al., 2014, 2017; Zhu et al., 2017), drug resistance (Bian et al., 2019; Gao et al., 2014; Lin, Xie, Lu, Hu, & Chang, 2018; Pan, Chen, Shen, & Tantai, 2019; Su et al., 2016; Xu et al., 2017; Zhou, Wang, & Feng, 2014), radiosensitivity (Liu, Li, & Gao, 2016), recurrence (Sim et al., 2018) or autophagy (Pan et al., 2019) in lung cancer, were identified (Table 4).

4 | DISCUSSION

To determine more possible targets for the exploration of SCLC and LCNEC biomarkers and molecular mechanisms, integrated bioinformatics methods based on the GSE1037 profile dataset were performed in the present study. Eighteen primary normal lung tissues, 8 primary LCNEC tissues, 15 primary SCLC tissues, and 9 SCLC cell lines were enrolled and analyzed. Using GEO2R and

TABLE 2 Enriched Go terms of the DEGs

	Category	Term	Count	%	*p*-Value	FDR
Up regulated	GOTERM_BP_DIRECT	GO:0051301~cell division	6	0.142993327	4.04E-06	0.004971483
	GOTERM_BP_DIRECT	GO:0006355~regulation of transcription DNA-templated	7	0.166825548	3.53E-04	0.432578524
	GOTERM_BP_DIRECT	GO:0006281~DNA repair	4	0.095328885	8.15E-04	0.997007591
	GOTERM_BP_DIRECT	GO:0045143~homologous chromosome segregation	2	0.047664442	.006639221	7.86341138
	GOTERM_BP_DIRECT	GO:0031536~positive regulation of exit from mitosis	2	0.047664442	.008292426	9.731016783
	GOTERM_BP_DIRECT	GO:0007067~mitotic nuclear division	3	0.071496663	.013030094	14.89218414
	GOTERM_BP_DIRECT	GO:0046323~glucose import	2	0.047664442	.018156528	20.17047326
	GOTERM_BP_DIRECT	GO:0051276~chromosome organization	2	0.047664442	.023053317	24.9298377
	GOTERM_BP_DIRECT	GO:0070979~protein K11-linked ubiquitination	2	0.047664442	.037603917	37.57710332
	GOTERM_BP_DIRECT	GO:0007052~mitotic spindle organization	2	0.047664442	.037603917	37.57710332
	GOTERM_BP_DIRECT	GO:0090307~mitotic spindle assembly	2	0.047664442	.045597774	43.66110836
	GOTERM_CC_DIRECT	GO:0005737~cytoplasm	15	0.357483317	2.21E-05	0.022280174
	GOTERM_CC_DIRECT	GO:0005634~nucleus	14	0.333651096	5.40E-05	0.054460588
	GOTERM_CC_DIRECT	GO:0043203~axon hillock	2	0.047664442	.00741693	7.237425098
	GOTERM_CC_DIRECT	GO:0032133~chromosome passenger complex	2	0.047664442	.00741693	7.237425098
	GOTERM_CC_DIRECT	GO:0005654~nucleoplasm	7	0.166825548	.010502317	10.10650713
	GOTERM_CC_DIRECT	GO:0045120~pronucleus	2	0.047664442	.013312558	12.64989615
	GOTERM_CC_DIRECT	GO:0051233~spindle midzone	2	0.047664442	.022093237	20.18460143
	GOTERM_MF_DIRECT	GO:0031625~ubiquitin protein ligase binding	3	0.076628352	.011662791	10.93819391
	GOTERM_MF_DIRECT	GO:0008301~DNA binding bending	2	0.051085568	.015851015	14.59560577
	GOTERM_MF_DIRECT	GO:0005524~ATP binding	6	0.153256705	.027091606	23.75384229
	GOTERM_MF_DIRECT	GO:0030414~peptidase inhibitor activity	2	0.051085568	.030054212	26.01571812
	GOTERM_MF_DIRECT	GO:0061631~ubiquitin conjugating enzyme activity	2	0.051085568	.038482685	32.12464677
Down regulated	GOTERM_BP_DIRECT	GO:0070836~caveola assembly	3	0.046260601	6.99E−05	0.098559412
	GOTERM_BP_DIRECT	GO:0007155~cell adhesion	6	0.092521203	.007419687	9.977332032
	GOTERM_BP_DIRECT	GO:0019065~receptor-mediated endocytosis of virus by host cell	2	0.030840401	.008018493	10.74080337
	GOTERM_BP_DIRECT	GO:0042420~dopamine catabolic process	2	0.030840401	.013329193	17.25342044
	GOTERM_BP_DIRECT	GO:0042135~neurotransmitter catabolic process	2	0.030840401	.021243157	26.14357095
	GOTERM_BP_DIRECT	GO:0050891~multicellular organismal water homeostasis	2	0.030840401	.021243157	26.14357095
	GOTERM_BP_DIRECT	GO:0001525~angiogenesis	4	0.061680802	.021777665	26.71078904
	GOTERM_BP_DIRECT	GO:0032060~bleb assembly	2	0.030840401	.026484616	31.53390357
	GOTERM_BP_DIRECT	GO:0006069~ethanol oxidation	2	0.030840401	.031698626	36.53140253
	GOTERM_BP_DIRECT	GO:0015793~glycerol transport	2	0.030840401	.034295382	38.89185575

(Continues)

TABLE 2 (Continued)

Category	Term	Count	%	*p*-Value	FDR
GOTERM_BP_DIRECT	GO:0009992~cellular water homeostasis	2	0.030840401	.034295382	38.89185575
GOTERM_CC_DIRECT	GO:0070062~extracellular exosome	16	0.246723207	.001317986	1.408901211
GOTERM_CC_DIRECT	GO:0005886~plasma membrane	19	0.292983809	.003743762	3.955034143
GOTERM_CC_DIRECT	GO:0005901~caveola	3	0.046260601	.010295194	10.53630766
GOTERM_CC_DIRECT	GO:0005576~extracellular region	10	0.154202005	.01150877	11.70950819
GOTERM_CC_DIRECT	GO:0045121~membrane raft	4	0.061680802	.012603718	12.75603307
GOTERM_CC_DIRECT	GO:0045177~apical part of cell	3	0.046260601	.013532583	13.63498448
GOTERM_CC_DIRECT	GO:0016021~integral component of membrane	20	0.308404009	.018955008	18.60768595
GOTERM_CC_DIRECT	GO:0031012~extracellular matrix	4	0.061680802	.032469722	29.89178143
GOTERM_CC_DIRECT	GO:0005615~extracellular space	8	0.123361604	.036771948	33.17391345
GOTERM_CC_DIRECT	GO:0002080~acrosomal membrane	2	0.030840401	.043912815	38.31524409
GOTERM_MF_DIRECT	GO:0016491~oxidoreductase activity	4	0.061680802	.014279333	14.99791487
GOTERM_MF_DIRECT	GO:0005215~transporter activity	4	0.061680802	.014662761	15.37073704
GOTERM_MF_DIRECT	GO:0004024~alcohol dehydrogenase activity zinc-dependent	2	0.030840401	.015188693	15.87969632
GOTERM_MF_DIRECT	GO:0005372~water transmembrane transporter activity	2	0.030840401	.015188693	15.87969632
GOTERM_MF_DIRECT	GO:0008131~primary amine oxidase activity	2	0.030840401	.015188693	15.87969632
GOTERM_MF_DIRECT	GO:0015254~glycerol channel activity	2	0.030840401	.030151975	29.24210187
GOTERM_MF_DIRECT	GO:0015250~water channel activity	2	0.030840401	.040003884	36.95130237

Abbreviations: DEGs, differentially expressed genes; Go, Gene ontology.

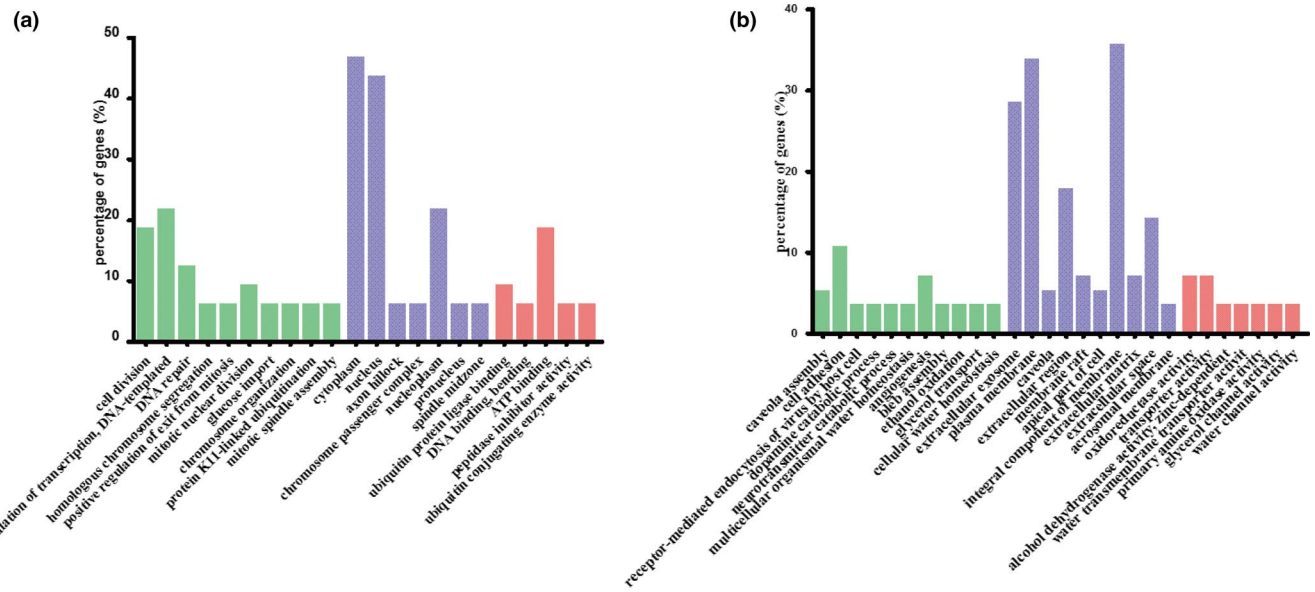

FIGURE 4 GO terms of overlapped differentially expressed genes. (a) Up-regulated genes. (b) Down-regulated genes. Green bars, biological process; blue bars, cellular component; red bars, molecular function. GO, Gene ontology

Venn tools, 88 common DEGs were detected (|logFC| > 2, adjusted $p < .05$) in SCLC and LCNEC, including 32 up-(|logFC < 0) and 56 downregulated DEGs (|logFC < 0). Subsequently, functional enrichment and GO analysis were performed by DAVID, which showed the following: (a) For BP, the significantly enriched terms of up-regulated DEGs

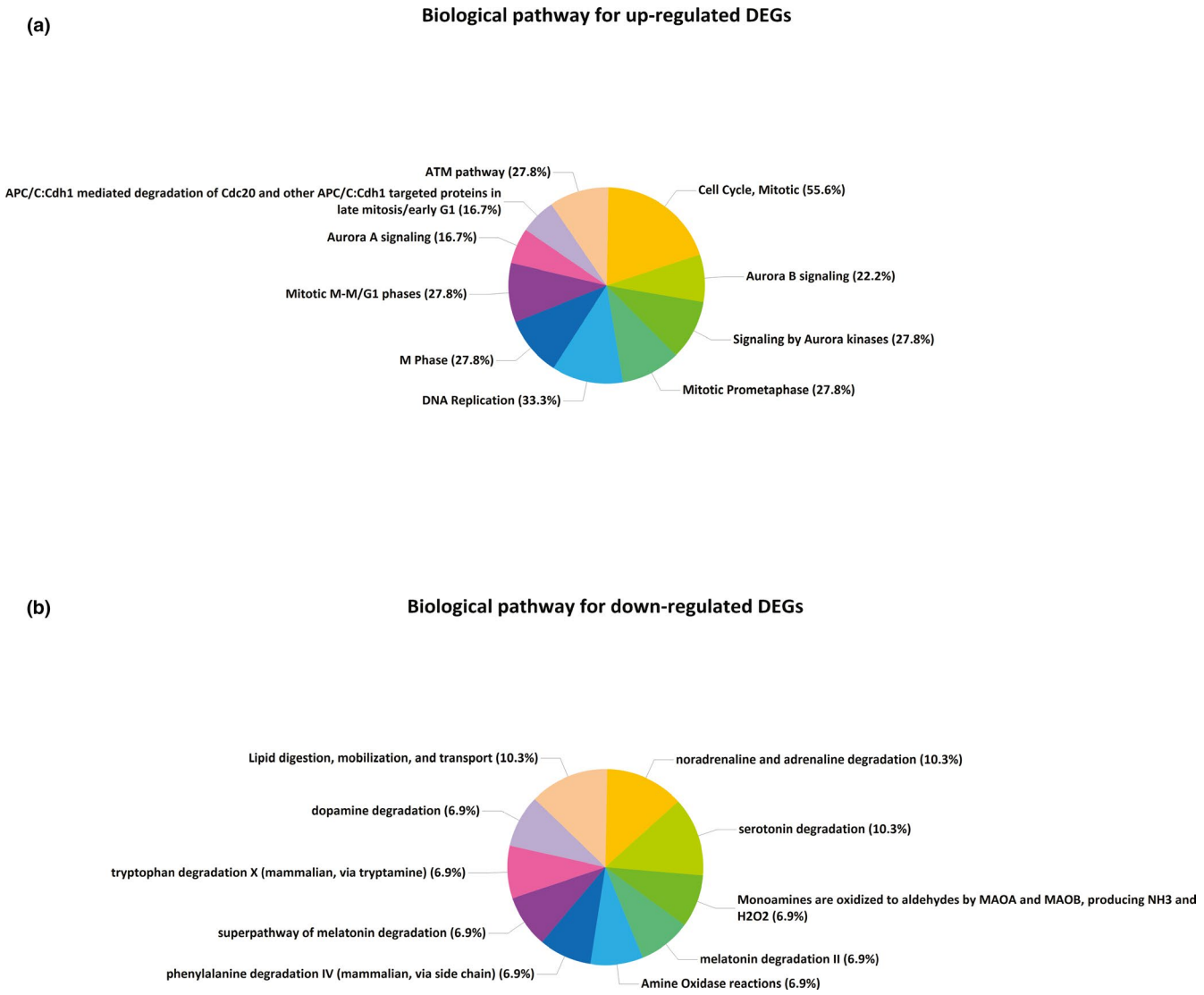

FIGURE 5 Biological pathway analysis for DEGs. (a) Biological pathways for upregulated DEGs. (b) Biological pathways for downregulated DEGs. DEGs, differentially expressed genes

were cell division, regulation of transcription, DNA repair, homologous chromosome segregation, positive regulation of exit from mitosis, mitotic nuclear division, glucose import, chromosome organization, protein K11-linked ubiquitination, mitotic spindle organization and mitotic spindle assembly, and the significantly enriched terms of downregulated DEGs were caveola assembly, cell adhesion, receptor-mediated endocytosis of virus by host cell, dopamine catabolic process, neurotransmitter catabolic process, multicellular organismal water homeostasis, angiogenesis, bleb assembly, ethanol oxidation, glycerol transport, and cellular water homeostasis; (b) for MF, the notably enriched terms of upregulated DEGs were ubiquitin protein ligase binding, DNA binding, ATP binding, peptidase inhibitor activity and ubiquitin conjugating enzyme activity, and those of downregulated DEGs were oxidoreductase, transporter, alcohol dehydrogenase (zinc-dependent), water transmembrane transporter, primary amine oxidase, glycerol channel and water channel activities; (c) for CC, upregulated DEGs were particularly enriched in the cytoplasm, nucleus, axon hillock, chromosome passenger complex, nucleoplasm, pronucleus and spindle midzone, and down-regulated DEGs in extracellular exosome, plasma membrane, caveola, extracellular region, membrane raft, apical part of cell, integral component of membrane, extracellular matrix, extracellular space and acrosomal membrane. To further explore the role of DEGs in biological pathways, the FunRich database was used. It was revealed that upregulated DEGs were notably enriched in the cell cycle pathway (mitotic), DNA replication, ATM pathway, mitotic M-M/G1 phases, signaling by Aurora kinases, M phase, and mitotic prometaphase, while downregulated DEGs in lipid digestion, mobilization transport, noradrenaline and adrenaline degradation, and serotonin degradation.

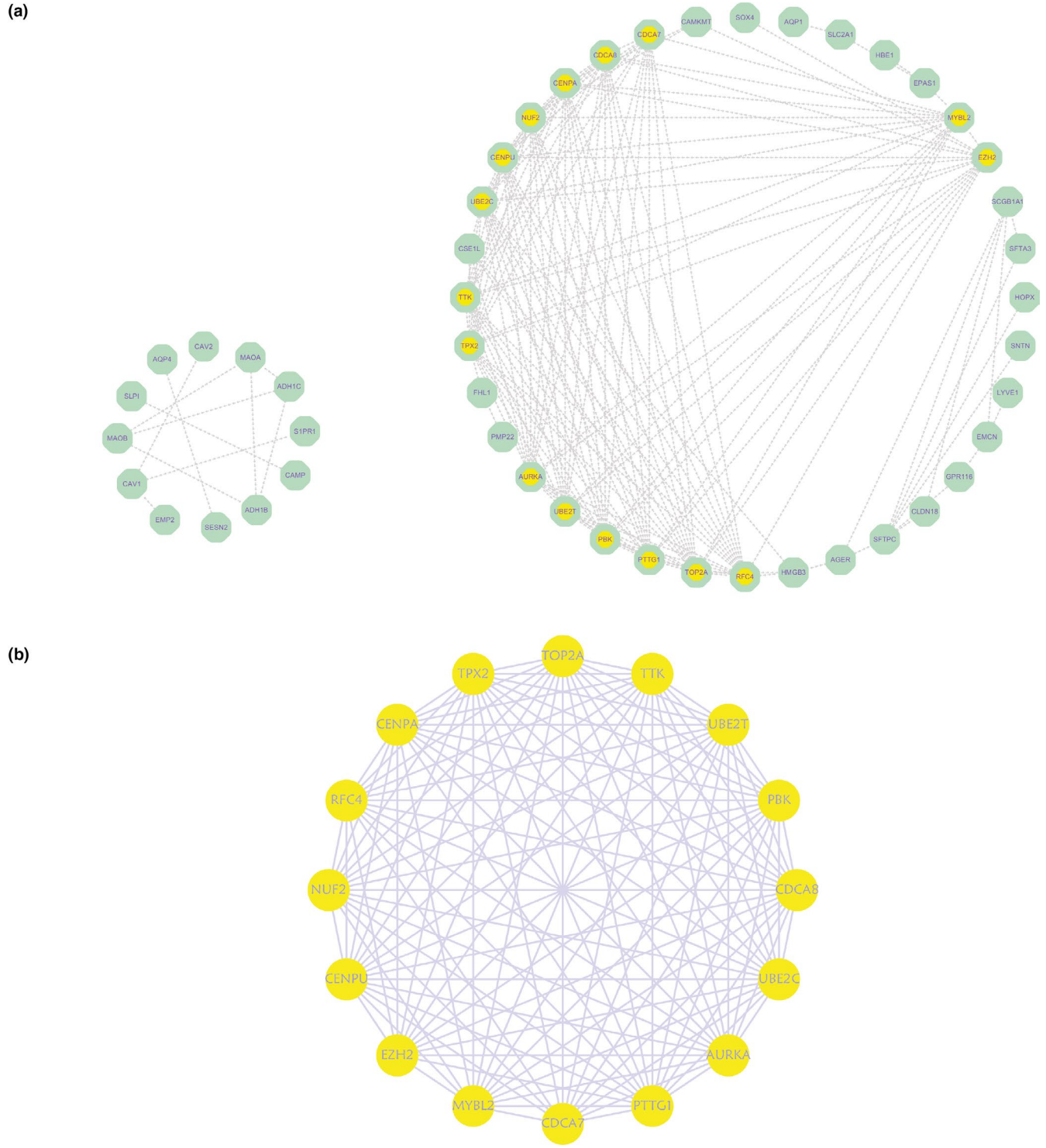

FIGURE 6 Common DEGs PPI network constructed by STRING online database and Module analysis. (a) There were a total of 48 DEGs in the DEGs PPI network complex. (b) The most significant module in the PPI network of the DEGs Module analysis of Cytoscape software (degree cutoff = 2, node score cutoff = 0.2, k-core = 2, and max. depth = 100). The nodes meant proteins; the edges meant the interaction of proteins; yellow nodes meant DEGs with high marks. DEGs, differentially expressed genes

A PPI network complex of 48 nodes with 221 edges was then generated using STRING and Cytoscape. Next, 16 key upregulated genes were selected by MCODE analysis. Furthermore, following a re-analysis of biological pathways by FunRich, 10 genes (*CDCA1, CDCA8, AURKA, RFC4, UBE2C, CENPA, CENPU, MYBL2, PTTG1,* and *TOP2A*) enriched in the cell cycle pathway were screened. In the meantime, target miRNAs associated with hub genes were predicted, and 8 genes (*TTK, PTTG1, MYBL2, EZH2, CENPA, CDCA8, CDCA7,* and *AURKA*) and 51 miRNAs

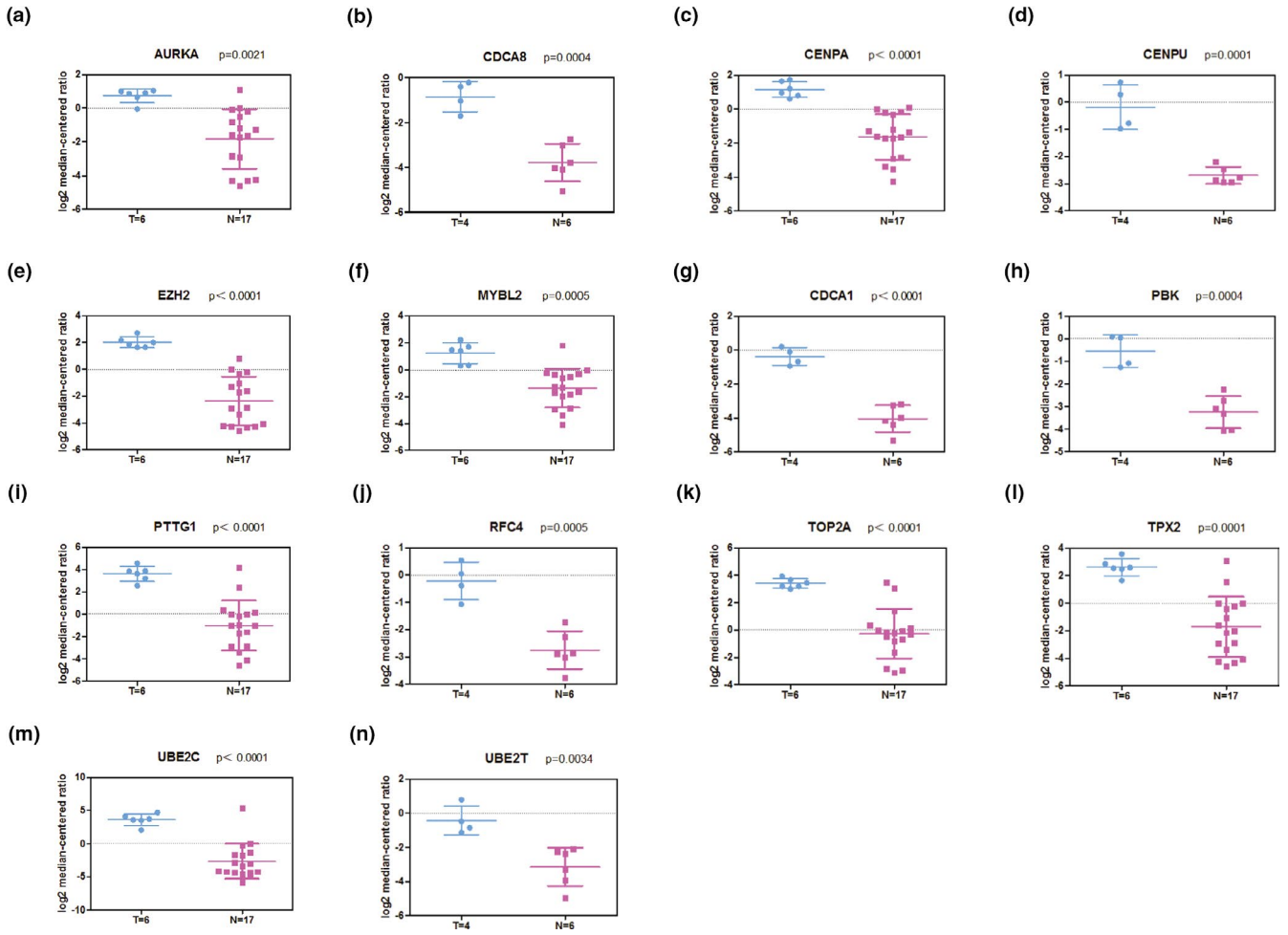

FIGURE 7 Significantly expressed 14 genes in SCLC tissues, as compared with normal tissues. SCLC, small cell lung carcinoma

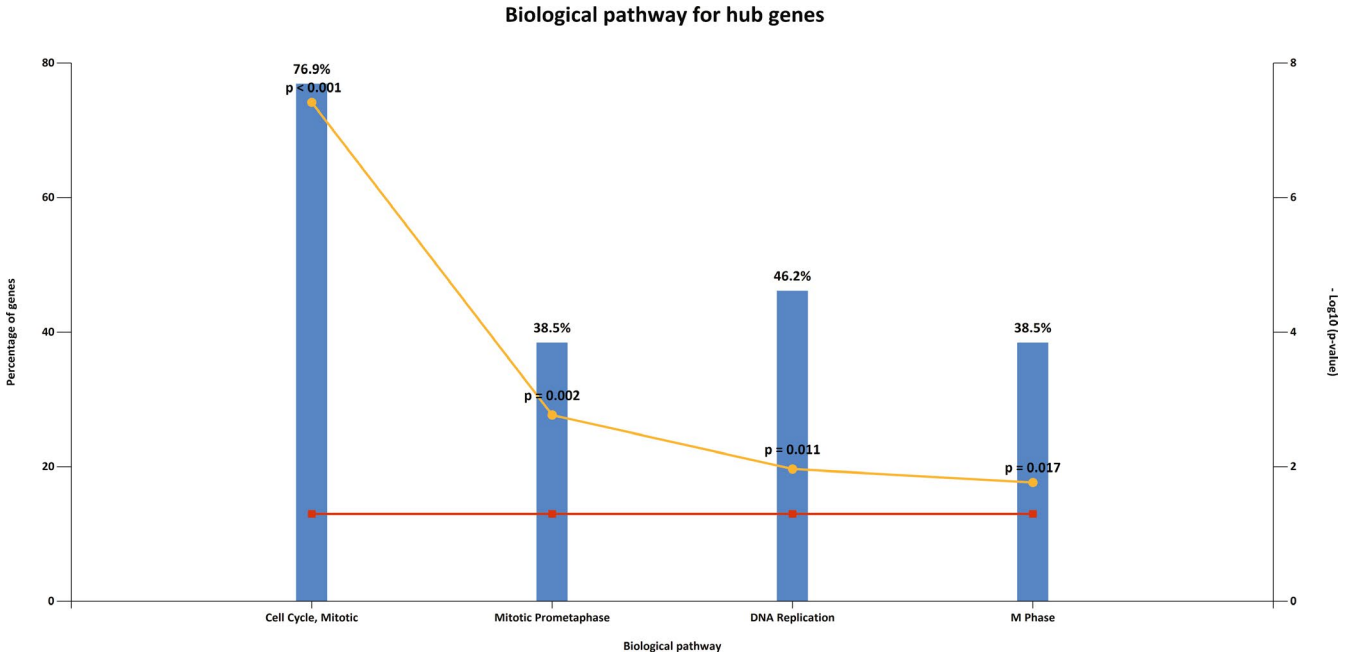

FIGURE 8 Re-analysis of 16 hub genes by biological pathway enrichment. X axis represents significant biological pathway terms; Y axis represents percentage of genes or –log10 (*p*-value)

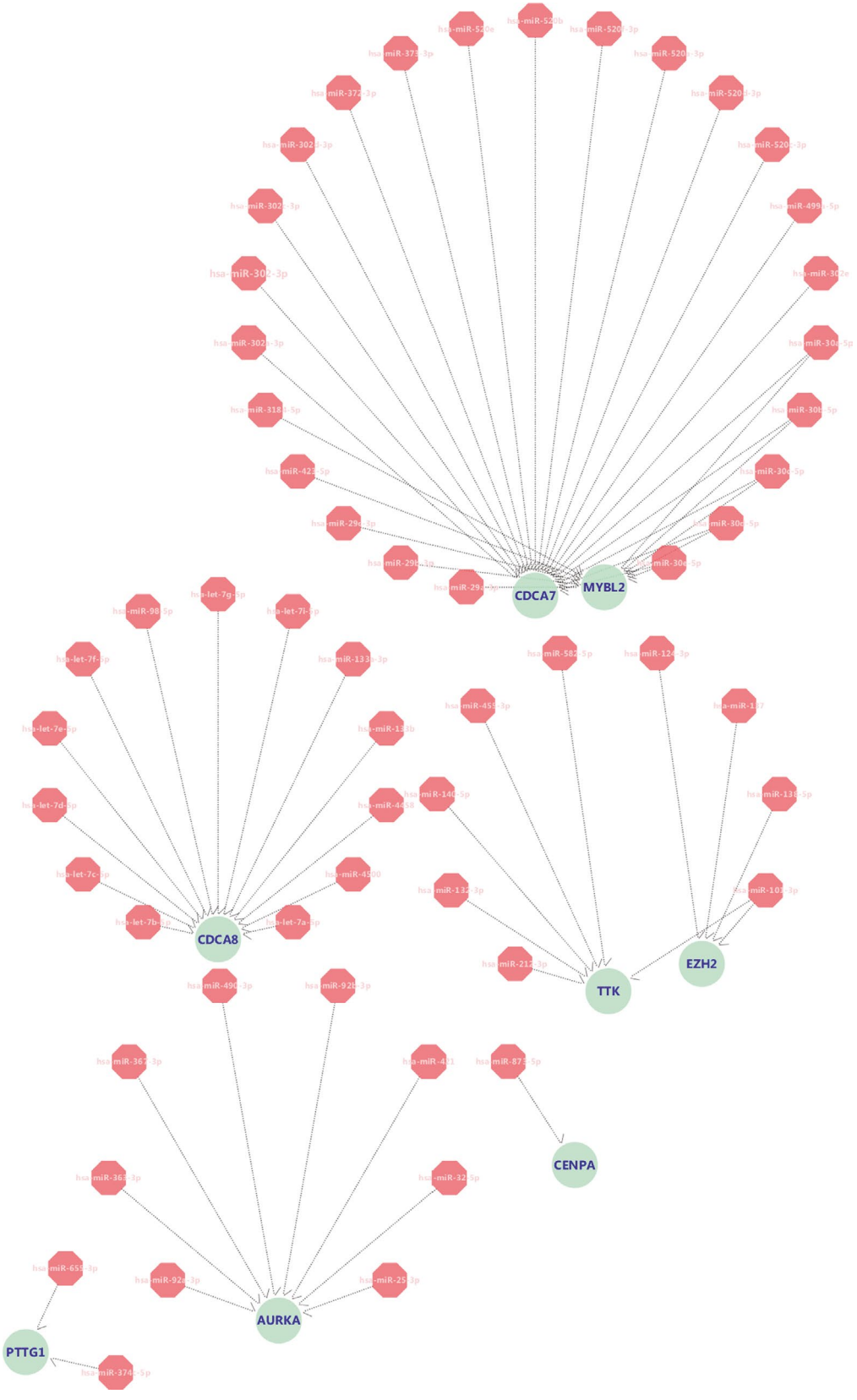

FIGURE 9 Target gene-miRNA networks of hub genes. Blue node stands for 8 hub genes, pink node stands for miRNA. The network was visualized by Cytoscape

TABLE 3 Hub genes and corresponded target miRNAs

Gene	miRNA
TTK	hsa-miR-101-3p hsa-miR-212-3p hsa-miR-132-3p hsa-miR-140-5p hsa-miR-455-3p hsa-miR-582-5p
PTTG1	hsa-miR-655-3p hsa-miR-374c-5p
MYBL2	hsa-miR-29a-3p hsa-miR-29b-3p hsa-miR-30c-5p hsa-miR-30a-5p hsa-miR-30b-5p hsa-miR-30d-5p hsa-miR-29c-3p hsa-miR-30e-5p hsa-miR-423-5p hsa-miR-3184-5p
EZH2	hsa-miR-101-3p hsa-miR-124-3p hsa-miR-137 hsa-miR-138-5p
CENPA	hsa-miR-873-5p
CDCA8	hsa-let-7a-5p hsa-let-7b-5p hsa-let-7c-5p hsa-let-7d-5p hsa-let-7e-5p hsa-let-7f-5p hsa-miR-98-5p hsa-let-7g-5p hsa-let-7i-5p hsa-miR-133a-3p hsa-miR-133b hsa-miR-4458 hsa-miR-4500
CDCA7	hsa-miR-30a-5p hsa-miR-30b-5p hsa-miR-30c-5p hsa-miR-30d-5p hsa-miR-30e-5p hsa-miR-302a-3p hsa-miR-302-3p hsa-miR-302c-3p hsa-miR-302d-3p hsa-miR-372-3p hsa-miR-373-3p hsa-miR-520e hsa-miR-520b hsa-miR-520f-3p hsa-miR-520a-3p hsa-miR-520d-3p hsa-miR-520c-3p hsa-miR-499a-5p hsa-miR-302e
AURKA	hsa-miR-25-3p hsa-miR-92a-3p hsa-miR-363-3p hsa-miR-367-3p hsa-miR-490-3p hsa-miR-92b-3p hsa-miR-421 hsa-miR-32-5p

TABLE 4 Functions of miRNAs in lung cancer

Gene	miRNA
TTK	hsa-miR-101-3p hsa-miR-212-3p hsa-miR-132-3p hsa-miR-140-5p hsa-miR-455-3p hsa-miR-582-5p
PTTG1	hsa-miR-655-3p hsa-miR-374c-5p
MYBL2	hsa-miR-29a-3p hsa-miR-29b-3p hsa-miR-30c-5p hsa-miR-30a-5p hsa-miR-30b-5p hsa-miR-30d-5p hsa-miR-29c-3p hsa-miR-30e-5p hsa-miR-423-5p hsa-miR-3184-5p
EZH2	hsa-miR-101-3p hsa-miR-124-3p hsa-miR-137 hsa-miR-138-5p
CENPA	hsa-miR-873-5p
CDCA8	hsa-let-7a-5p hsa-let-7b-5p hsa-let-7c-5p hsa-let-7d-5p hsa-let-7e-5p hsa-let-7f-5p hsa-miR-98-5p hsa-let-7g-5p hsa-let-7i-5p hsa-miR-133a-3p hsa-miR-133b hsa-miR-4458 hsa-miR-4500
CDCA7	hsa-miR-30a-5p hsa-miR-30b-5p hsa-miR-30c-5p hsa-miR-30d-5p hsa-miR-30e-5p hsa-miR-302a-3p hsa-miR-302-3p hsa-miR-302c-3p hsa-miR-302d-3p hsa-miR-372-3p hsa-miR-373-3p hsa-miR-520e hsa-miR-520b hsa-miR-520f-3p hsa-miR-520a-3p hsa-miR-520d-3p hsa-miR-520c-3p hsa-miR-499a-5p hsa-miR-302e
AURKA	hsa-miR-25-3p hsa-miR-92a-3p hsa-miR-363-3p hsa-miR-367-3p hsa-miR-490-3p hsa-miR-92b-3p hsa-miR-421 hsa-miR-32-5p

involved in the mRNA-miRNA regulatory network of SCLC and LCNEC were identified.

CDCA1, is a centromeric protein (Nabetani, Koujin, Tsutsumi, Haraguchi, & Hiraoka, 2001), also known as *NUF2*. The gene has been reported to be co-expressed with cell cycle-related genes, including *CDC2*, cyclin, *TOP2A*, and others (Walker, 2001), which was in line with the present results. It has been identified that the co-activation of *KNTC2* and *CDCA1* and their cognate interactions had an impact on pulmonary carcinogenesis, and that the inhibition of the *KNTC2-CDCA1* complex would provide a novel strategy for therapy of lung cancer treatment. *CDCA1* was also regarded as a potential interacting protein for ZW10, a prognostic marker for lung cancer (Hayama et al., 2006; Yuan et al., 2018). In addition, *CDCA1* is projected to be a candidate of tumor-associated antigens (TAA) in SCLC. *CDCA1*, with increasing levels in SCLC, could act as a TAA in inducing cytotoxic T lymphocytes (CTLs) which killed tumor cell lines, and therefore made differences in immunotherapy.(Harao et al., 2008).

CDCA8, a member of the chromosomal passenger complex, is indispensable for the transmission of the genome in the process of cell division (Hindriksen, Meppelink, & Lens, 2015). Bidkhori et al constructed a co-expression network and identified *CDCA8* as a crucial gene in lung adenocarcinoma (Bidkhori et al., 2013). Another study implied that the *CDCA8-AURKB* pathway participated in the process of lung carcinogenesis (Hayama et al., 2007). However, we failed to obtain studies of the impact of *CDCA8* neither in SCLC nor in LCNEC.

AURKA, a serine-threonine protein kinase, was found to be involved in several crucial mitotic events and was regarded as an oncogene in multiple types of cancer (Vader & Lens, 2008). In SCLC cell lines, a decreased level of *AURKA* inhibited cell proliferation and promoted apoptosis, and the inhibition of *AURKA* may be involved in the G2/M phase arrest of the cell cycle (Lu et al., 2014). Apart from that way, *AURKA* was involved in immunotherapy in SCLC by being regarded as a TAA to induce CTLs.(Babiak et al., 2014) Recently, more and more studies are concentrating on Aurora Kinase Inhibitors, PF-03814735 and AZD1152, which establishes its pivotal status of SCLC in vitro and vivo.(Helfrich et al., 2016; Hook et al., 2012) Studies have also underlined the role of *AURKA* in platinum-resistance as well as acquired resistance to third-generation EGFR inhibitors (both osimertinib and rociletinib) (Gay et al., 2019; Shah et al., 2019). In addition, *AURKA* was reportedly correlated with poor prognosis in smoking-related lung adenocarcinoma (Zhang, Hao, et al., 2018).

RFC4 is a member of the RFC family and has been found to be involved in DNA replication (Arai et al., 2009). In colorectal cancer, the forced expression of *RFC4* was associated

with tumor progression, poor prognosis (Xiang et al., 2014), and radioresistance (X. C. Wang, Yue, et al., 2019). *RFC4* knockdown in liver cancer cells could suppress proliferation and induce apoptosis (Arai et al., 2009). In lung adenocarcinoma, *RFC4* was regulated by an oncogene, protein kinases C (*PKC*)-iota, and correlated with the PKC-iota expression in several more tumor types (Erdogan, Klee, Thompson, & Fields, 2009).

UBE2C, a ubiquitin-conjugating enzyme, works with the ubiquitin-activating enzyme E1 and ubiquitin protein ligase E3 to degradate key regulatory molecules in cell cycle progression (Mayer, 2000). In addition, *UBE2C* intervened in the cell cycle, apoptosis and transcription processes and controlled tumoriogenesis. Previous studies have implied that *UBE2C* promotes cell growth (Jin et al., 2019; van Ree, Jeganathan, Malureanu, & van Deursen, 2010; Sivakumar et al., 2017) in NSCLC and is correlated with poor prognosis (Chen et al., 2011; Guo et al., 2017; Psyrri et al., 2012). In addition, UBE2C participated in the miR 495-*UBE2C-ABCG2/ERCC1* axis regulating cisplatin resistance and mediating autophagy in NSCLC (Guo, Jin, et al., 2018; Guo, Wu, et al., 2018).*UBE2C* were in similarly high level in small-cell prostate carcinoma (SCPC) and LCNEC of the prostate with xenografts, and the expression of *UBE2C* in SCLC and LCNEC of the lung might bear a strong resemblance to that of SCPC and LCNEC of the prostate (Tzelepi et al., 2012).

CENPA, a centromere-specific 17-kDa protein, is a crucial histone H3 variant that acts as a vital epigenetic mark for the identity and propagation of the centromere (Allshire & Karpen, 2008). *CENPA* played an essential role in cell cycle regulation and tumor cell survival (Takada et al., 2017). Recent studies have identified the impacts of *CENPA* in lung cancer. Liu et al. (2018) used integrated microarray analysis and confirmed *CENPA*, cyclin-dependent kinase 1, and cell-division cycle protein 20 as a cluster of prognostic biomarkers for patients with lung adenocarcinoma. It has also been revealed that *CENPA* intensifies the aggressive phenotype of lung adenocarcinoma and is associated with patient prognosis (Cheng et al., 2019; Wu et al., 2014, 2012).

CENPU, also known as *PBIP1/KLIP1/CENP-50/MLF1IP*, is indispensable for kinetochore-microtubule attachment, chromosome segregation, and recovery from spindle damage (Kagawa et al., 2014; Walter et al., 2015). Mounting evidence (Li, Zhang, Zhang, & Wang, 2018; Wang et al., 2017; Zhang et al., 2015) has indicated that *CENPU* influences several types of cancer, such as bladder and ovarian cancer, and prostate carcinoma. Furthermore, *CENPU* predicted poor survival in patients with lung carcinoma and affected lung tumor growth (Li, Wang, Pang, Zhang, & Wang, 2019; Wang et al., 2018; Zhang, Li, Zhang, & Shi, 2018).

MYBL2 participated in cell cycle regulation, cell survival, and EMT-associated processes in carcinoma (Musa, Aynaud, Mirabeau, Delattre, & Grunewald, 2017). Accumulating evidence has indicated that *MYBL2* regulated tumorigenesis and cancer progression in multiple types of cancer. The high expression of *MYBL2* disrupted the DREAM complex and then hindered the cell cycle process in breast and ovarian cancer (Iness et al., 2019). In liver cancer cells, YAP supported cell proliferation in an *MYBL2*-dependant manner (Wei et al., 2019). In addition, Fan et al. (2018) and Jin et al. (2017) stressed the oncogenic impacts of *MYBL2* and its capacity to serve as a therapeutic target in NSCLC. Moreover the overexpression of *MYBL2* was found to be related to that of the ubiquitin carboxyterminal hydrolase UCHL1 (an enzyme expressed in neurons and neuroendocrine cells in the lung) in murine, because of the reciprocal action of the UCHL1 enzyme and *MYBL2* (Long, Long, Tsirigotis, & Gray, 2003).

PTTG1 is a novel proto-oncogene that is overexpressed in different types of human cancers, including endocrine- and nonendocrine-related types (Vlotides, Eigler, & Melmed, 2007). Wu, Zhang, et al. (2019)) revealed the importance of *PTTG1* as a potential biomarker in NSCLC. Accordingly, Wang, Liu, and Chen (2016) emphasized the prognostic value of *PTTG1* in lung cancer, showing the level of PGGT1 as an optimal parameter to predict malignant status and prognosis in NSCLC patients.

TOP2A is a type of isozyme type II topoisomerases (Li & Liu, 2001). A dysregulated *TOP2A* has been observed in multiple types of cancer and been used in the treatment of several carcinomas (Lan et al., 2014; Li et al., 2015; Wesierska-Gadek & Skladanowski, 2012). *TOP2A* has been shown to be involved not only in NSCLC (Chien et al., 2019; Olaussen & Postel-Vinay, 2016), but also in SCLC (Chiappori et al., 2010). Chiappori et al. (2010) recommended *TOP2A* as a biomarker of chemotherapeutic efficacy in SCLC. Chang et al. (2017)) and Gray et al. (2017) considered *TOP2A* as a target of anti-small cell lung cancer agents. Furthermore, in silico analyses showed *TOP2A* as target gene of miR-27a-5p and miR-34b-3p, both of whom were tumor suppressors in SCLC (Mizuno et al., 2017). A current research showed that compared with lung adenocarcinoma, *TOP2A* was a potential drug target of the therapy in LCNEC due to its overexpression examined by immunohistochemistry (Makino et al., 2016). Although *TOP2A* was highly expressed in NENs, no evident difference in expression levels was found between SCLC and LCNEC (Neubauer et al., 2016).

The results of re-analysis of biological pathway revealed that most key genes were enriched in cell cycle (mitotic), mitotic prometaphase, DNA replication, and M phase. Accordingly, because of the high genome instability as a result of high level replication stress in SCLC, the inhibition

of DNA-replication stress-response, especially in combination with cisplatin, was one of the vulnerabilities of SCLC, which provided a novel therapy for this type of cancer (Bian & Lin, 2019; Nagel et al., 2019). Prometaphase arrest caused by mitotic spindle formation defects that resulting from the depletion of Aurora A, was also involved with the inhibition of cell growth in SCLC (Du et al., 2019). Additionally, the inhibition of a pivotal mitotic regulator led to the increase in the population of cells in the G2/M phase (Wang et al., 2018), while treatment with etoposide in TP53 gene abnormalities ones resulted in the lack of G1/S arrest (Soues, Wiltshire, & Smith, 2001), all of which were associated with pathways of mitotic cell cycle or M phase in SCLC cell lines.

To sum up, *CDCA1* and *AURK4* might be characteristic especially to SCLC, while *MYBL2* is the biomarker of LCNEC. The biological pathway of DNA replication, mitotic cell cycle, mitotic prometaphase, and M phase might be characteristic to SCLC. In contrast, no evidence has been shown that any pathway enrichment is related to LCNEC, and the genes of *CDCA8*, *RFC4*, *UBE2C*, *CENPA*, *CENPU*, *PTTG1,* and *TOP2A* are not predicted to participate particularly in SCLC or LCNEC. Although further researches should be performed focusing on more functions of these key genes and pathways, our discoveries provide potential candidates useful for the diagnosis and discrimination between SCLC and LCNEC.

miRNAs play essential roles in the genesis, development, and progression of carcinoma (Rupaimoole & Slack, 2017). Aberrant miRNA expression profiles have been identified in multiple subtypes of lung cancer (Lai et al., 2019; Mao et al., 2019; Wang et al., 2018). In addition to DEGs and their functions, miRNAs can influence multiple processes of lung cancer, including drug resistance, tumor progression and recurrence, autophagy and radio-sensitivity. The role of miRNAs in tumor growth is shown in Table 4. Recent studies have also revealed the impacts of miRNAs, including miR-363-3p, miR-30a-5p, miR-133b, miR-98-5p, miR-138-5p, miR-137, and miR-138-5p, on drug resistance in NSCLC, showing that miRNAs participated in the mechanisms of traditional chemotherapeutic drugs [gemcitabine (Bian et al., 2019), paclitaxel (Xu et al., 2017), and cisplatin (Lin et al., 2018; Pan et al., 2019; Su et al., 2016; Zhou et al., 2014)] as well as targeted drugs [gefitinib (Gao et al., 2014)]. In addition, Sim et al demonstrated that let-7g-5p was associated with recurrence in stage I lung adenocarcinoma (Sim et al., 2018). Other studies also elucidated the roles of miRNAs in autophagy and radio-sensitivity (Liu, Miao, et al., 2016; Pan et al., 2019).

However, the present study had several limitations. First, due to the rarity of LCNEC and SCLC, we failed to provide meaningful prognosis information from public databases. Second, the present data were obtained from the GEO database, so the reliability and quality of the statistics cannot be evaluated. Third, this study lacks more convincing evidence, such as qPCR and immunohistochemistry results.

5 | CONCLUSIONS

In conclusion, common DEGs of SCLC and LCNEC were identified by integrated bioinformatics methods and 16 hub genes were selected from PPI network, among which 10 genes were shown to be related to the most significantly enriched pathway, cell cycle pathway. The roles of these genes and pathways in lung cancer were further discussed and the application of these genes in treatment of SCLC and LCNEC is worthy of further study. In addition, the functions in lung cancer of miRNAs corresponding to 16 core genes were discussed. Several studies have tried to explore novel strategies (Christopoulos et al., 2017; Kujtan et al., 2018; Saunders et al., 2015) for the treatment of SCLC and LCNEC. Attempts at identifying the values of molecular targets, such as spread through air spaces, and immune therapy, such as the expression of PD-L1 and mutation burden, are ongoing (Aly et al., 2019; Kim et al., 2018). To determine the various roles of emerging molecules in the process of tumorigenesis and progression of SCLC and LCNEC, further research should be conducted.

ACKNOWLEDGMENTS

This work was supported by grants from the Natural Science Foundation of Shandong Province (No. ZR2017MH062) and the Science and Technology for People's Livelihood Project of Qingdao (No. 17-3-3-33-nsh).

CONFLICT OF INTEREST

None declared.

ORCID

Zhuang Yu https://orcid.org/0000-0003-1676-135X

REFERENCES

Allshire, R. C., & Karpen, G. H. (2008). Epigenetic regulation of centromeric chromatin: Old dogs, new tricks? *Nature Reviews Genetics*, *9*(12), 923–937. https://doi.org/10.1038/nrg2466

Aly, R. G., Rekhtman, N., Li, X., Takahashi, Y., Eguchi, T., Tan, K. S., … Travis, W. D. (2019). Spread through air spaces (STAS) is prognostic in atypical carcinoid, large cell neuroendocrine carcinoma, and small cell carcinoma of the lung. *Journal of Thoracic Oncology*, *14*(9), 1583–1593. https://doi.org/10.1016/j.jtho.2019.05.009

Arai, M., Kondoh, N., Imazeki, N., Hada, A., Hatsuse, K., Matsubara, O., & Yamamoto, M. (2009). The knockdown of endogenous replication factor C4 decreases the growth and enhances the chemosensitivity of hepatocellular carcinoma cells. *Liver International: Official Journal of the International Association for the Study of the Liver*, *29*(1), 55–62. https://doi.org/10.1111/j.1478-3231.2008.01792.x

Asamura, H., Kameya, T., Matsuno, Y., Noguchi, M., Tada, H., Ishikawa, Y., … Nagai, K. (2006). Neuroendocrine neoplasms of the lung: A prognostic spectrum. *Journal of Clinical Oncology*, *24*(1), 70–76. https://doi.org/10.1200/jco.2005.04.1202

Babiak, A., Steinhauser, M., Gotz, M., Herbst, C., Dohner, H., & Greiner, J. (2014). Frequent T cell responses against immunogenic

targets in lung cancer patients for targeted immunotherapy. *Oncology Reports*, *31*(1), 384–390. https://doi.org/10.3892/or.2013.2804

Bhattacharjee, A., Richards, W. G., Staunton, J., Li, C., Monti, S., Vasa, P., … Meyerson, M. (2001). Classification of human lung carcinomas by mRNA expression profiling reveals distinct adenocarcinoma subclasses. *Proceedings of the National Academy of Sciences of the United States of America*, *98*(24), 13790–13795. https://doi.org/10.1073/pnas.191502998

Bian, W. G., Zhou, X. N., Song, S., Chen, H. T., Shen, Y., & Chen, P. (2019). Reduced miR-363-3p expression in non-small cell lung cancer is associated with gemcitabine resistance via targeting of CUL4A. *European Review for Medical and Pharmacological Sciences*, *23*(2), 649–659. https://doi.org/10.26355/eurrev_201901_16879

Bian, X., & Lin, W. (2019). Targeting DNA replication stress and DNA double-strand break repair for optimizing SCLC Treatment. *Cancers (Basel)*, *11*(9), https://doi.org/10.3390/cancers11091289

Bidkhori, G., Narimani, Z., Hosseini Ashtiani, S., Moeini, A., Nowzari-Dalini, A., & Masoudi-Nejad, A. (2013). Reconstruction of an integrated genome-scale co-expression network reveals key modules involved in lung adenocarcinoma. *PLoS ONE*, *8*(7), e67552. https://doi.org/10.1371/journal.pone.0067552

Cerilli, L. A., Ritter, J. H., Mills, S. E., & Wick, M. R. (2001). Neuroendocrine neoplasms of the lung. *American Journal of Clinical Pathology*, *116*(Suppl), S65–S96. https://doi.org/10.1309/bpy4-vgtb-patf-vuxu

Chang, J., Gao, F., Chu, H., Lou, L., Wang, H., & Chen, Y. (2019). miR-363-3p inhibits migration, invasion, and epithelial-mesenchymal transition by targeting NEDD9 and SOX4 in non-small-cell lung cancer. *Journal of Cellular Physiology*, *235*(2), 1808–1820. https://doi.org/10.1002/jcp.29099

Chang, T.-H., Tsai, M.-F., Gow, C.-H., Wu, S.-G., Liu, Y.-N., Chang, Y.-L., … Shih, J.-Y. (2017). Upregulation of microRNA-137 expression by Slug promotes tumor invasion and metastasis of non-small cell lung cancer cells through suppression of TFAP2C. *Cancer Letters*, *402*, 190–202. https://doi.org/10.1016/j.canlet.2017.06.002

Chen, D. I., Guo, W., Qiu, Z., Wang, Q., Li, Y., Liang, L., … He, X. (2015). MicroRNA-30d-5p inhibits tumour cell proliferation and motility by directly targeting CCNE2 in non-small cell lung cancer. *Cancer Letters*, *362*(2), 208–217. https://doi.org/10.1016/j.canlet.2015.03.041

Chen, Z., Zhang, C., Wu, D., Chen, H., Rorick, A., Zhang, X., & Wang, Q. (2011). Phospho-MED1-enhanced UBE2C locus looping drives castration-resistant prostate cancer growth. *EMBO Journal*, *30*(12), 2405–2419. https://doi.org/10.1038/emboj.2011.154

Cheng, Z., Yu, C., Cui, S., Wang, H., Jin, H., Wang, C., … Qin, W. (2019). circTP63 functions as a ceRNA to promote lung squamous cell carcinoma progression by upregulating FOXM1. *Nature Communications*, *10*(1), 3200. https://doi.org/10.1038/s41467-019-11162-4

Chiappori, A. A., Zheng, Z., Chen, T., Rawal, B., Schell, M. J., Mullaney, B. P., & Bepler, G. (2010). Features of potentially predictive biomarkers of chemotherapeutic efficacy in small cell lung cancer. *Journal of Thoracic Oncology*, *5*(4), 484–490. https://doi.org/10.1097/JTO.0b013e3181ccb27b

Chien, C.-M., Yang, J.-C., Wu, P.-H., Wu, C.-Y., Chen, G.-Y., Wu, Y.-C., … Chiu, C.-C. (2019). Phytochemical naphtho[1,2-b] furan-4,5di-one induced topoisomerase II-mediated DNA damage response in human non-small-cell lung cancer. *Phytomedicine*, *54*, 109–119. https://doi.org/10.1016/j.phymed.2018.06.025

Christopoulos, P., Engel-Riedel, W., Grohé, C., Kropf-Sanchen, C., von Pawel, J., Gütz, S., … Thomas, M. (2017). Everolimus with paclitaxel and carboplatin as first-line treatment for metastatic large-cell neuroendocrine lung carcinoma: A multicenter phase II trial. *Annals of Oncology*, *28*(8), 1898–1902. https://doi.org/10.1093/annonc/mdx268

Clinical Lung Cancer Genome Project (CLCGP); Network Genomic Medicine (NGM). (2013). A genomics-based classification of human lung tumors. *Science Translational Medicine*, *5*(209), 209ra153. https://doi.org/10.1126/scitranslmed.3006802

Davis, S., & Meltzer, P. S. (2007). GEOquery: A bridge between the Gene Expression Omnibus (GEO) and BioConductor. *Bioinformatics*, *23*(14), 1846–1847. https://doi.org/10.1093/bioinformatics/btm254

Du, J., Yan, L., Torres, R., Gong, X., Bian, H., Marugán, C., … Campbell, R. M. (2019). Aurora A-selective inhibitor LY3295668 leads to dominant mitotic arrest, apoptosis in cancer cells, and shows potent preclinical antitumor efficacy. *Molecular Cancer Therapeutics*, *18*(12), 2207–2219. https://doi.org/10.1158/1535-7163.mct-18-0529

Erdogan, E., Klee, E. W., Thompson, E. A., & Fields, A. P. (2009). Meta-analysis of oncogenic protein kinase Ciota signaling in lung adenocarcinoma. *Clinical Cancer Research*, *15*(5), 1527–1533. https://doi.org/10.1158/1078-0432.ccr-08-2459

Fan, X., Wang, Y., Jiang, T., Cai, W., Jin, Y., Niu, Y., Bu, Y. (2018). B-Myb mediates proliferation and migration of non-small-cell lung cancer via suppressing IGFBP3. *International Journal of Molecular Sciences*, *19*(5), 1479. https://doi.org/10.3390/ijms19051479

Gao, X., Zhao, H., Diao, C., Wang, X., Xie, Y., Liu, Y., … Zhang, M. (2018). miR-455-3p serves as prognostic factor and regulates the proliferation and migration of non-small cell lung cancer through targeting HOXB5. *Biochemical and Biophysical Research Communications*, *495*(1), 1074–1080. https://doi.org/10.1016/j.bbrc.2017.11.123

Gao, Y., Fan, X., Li, W., Ping, W., Deng, Y., & Fu, X. (2014). miR-138-5p reverses gefitinib resistance in non-small cell lung cancer cells via negatively regulating G protein-coupled receptor 124. *Biochemical and Biophysical Research Communications*, *446*(1), 179–186. https://doi.org/10.1016/j.bbrc.2014.02.073

Garber, M. E., Troyanskaya, O. G., Schluens, K., Petersen, S., Thaesler, Z., Pacyna-Gengelbach, M., … Petersen, I. (2001). Diversity of gene expression in adenocarcinoma of the lung. *Proceedings of the National Academy of Sciences of the United States of America*, *98*(24), 13784–13789. https://doi.org/10.1073/pnas.241500798

Gay, C. M., Tong, P., Cardnell, R. J., Sen, T., Su, X., Ma, J., … Byers, L. A. (2019). Differential sensitivity analysis for resistant malignancies (DISARM) identifies common candidate therapies across platinum-resistant cancers. *Clinical Cancer Research*, *25*(1), 346–357. https://doi.org/10.1158/1078-0432.ccr-18-1129

Gray, J. E., Heist, R. S., Starodub, A. N., Camidge, D. R., Kio, E. A., Masters, G. A., … Goldenberg, D. M. (2017). Therapy of small cell lung cancer (SCLC) with a topoisomerase-I-inhibiting antibody-drug conjugate (ADC) targeting trop-2. *Sacituzumab Govitecan. Clin Cancer Res*, *23*(19), 5711–5719. https://doi.org/10.1158/1078-0432.ccr-17-0933

Gu, H., Yang, T., Fu, S., Chen, X., Guo, L., & Ni, Y. (2014). MicroRNA-490-3p inhibits proliferation of A549 lung cancer cells by targeting CCND1. *Biochemical and Biophysical Research Communications*, *444*(1), 104–108. https://doi.org/10.1016/j.bbrc.2014.01.020

Guo, J., Jin, D., Wu, Y., Yang, L., Du, J., Gong, K., … Xi, S. (2018). The miR 495-UBE2C-ABCG2/ERCC1 axis reverses cisplatin resistance

by downregulating drug resistance genes in cisplatin-resistant non-small cell lung cancer cells. *EBioMedicine*, *35*, 204–221. https://doi.org/10.1016/j.ebiom.2018.08.001

Guo, J., Wu, Y., Du, J., Yang, L., Chen, W., Gong, K., … Xi, S. (2018). Deregulation of UBE2C-mediated autophagy repression aggravates NSCLC progression. *Oncogenesis*, *7*(6), 49. https://doi.org/10.1038/s41389-018-0054-6

Guo, L., Ding, Z., Huang, N., Huang, Z., Zhang, N., & Xia, Z. (2017). Forkhead Box M1 positively regulates UBE2C and protects glioma cells from autophagic death. *Cell Cycle*, *16*(18), 1705–1718. https://doi.org/10.1080/15384101.2017.1356507

Han, C., Kawata, M., Hamada, Y., Kondo, T., Wada, J., Asano, K., … Narita, M. (2019). Analyses of the possible anti-tumor effect of yokukansan. *Journal of Natural Medicines*, *73*(3), 468–479. https://doi.org/10.1007/s11418-019-01283-x

Harao, M., Hirata, S., Irie, A., Senju, S., Nakatsura, T., Komori, H., … Nishimura, Y. (2008). HLA-A2-restricted CTL epitopes of a novel lung cancer-associated cancer testis antigen, cell division cycle associated 1, can induce tumor-reactive CTL. *International Journal of Cancer*, *123*(11), 2616–2625. https://doi.org/10.1002/ijc.23823

Hayama, S., Daigo, Y., Kato, T., Ishikawa, N., Yamabuki, T., Miyamoto, M., … Nakamura, Y. (2006). Activation of CDCA1-KNTC2, members of centromere protein complex, involved in pulmonary carcinogenesis. *Cancer Research*, *66*(21), 10339–10348. https://doi.org/10.1158/0008-5472.can-06-2137

Hayama, S., Daigo, Y., Yamabuki, T., Hirata, D., Kato, T., Miyamoto, M., … Nakamura, Y. (2007). Phosphorylation and activation of cell division cycle associated 8 by aurora kinase B plays a significant role in human lung carcinogenesis. *Cancer Research*, *67*(9), 4113–4122. https://doi.org/10.1158/0008-5472.can-06-4705

He, S., Li, Z., Yu, Y., Zeng, Q., Cheng, Y., Ji, W., … Lu, S. (2019). Exosomal miR-499a-5p promotes cell proliferation, migration and EMT via mTOR signaling pathway in lung adenocarcinoma. *Experimental Cell Research*, *379*(2), 203–213. https://doi.org/10.1016/j.yexcr.2019.03.035

Helfrich, B. A., Kim, J., Gao, D., Chan, D. C., Zhang, Z., Tan, A. C., & Bunn, P. A. (2016). Barasertib (AZD1152), a small molecule aurora B inhibitor, inhibits the growth of SCLC cell lines in vitro and in vivo. *Molecular Cancer Therapeutics*, *15*(10), 2314–2322. https://doi.org/10.1158/1535-7163.mct-16-0298

Hindriksen, S., Meppelink, A., & Lens, S. M. (2015). Functionality of the chromosomal passenger complex in cancer. *Biochemical Society Transactions*, *43*(1), 23–32. https://doi.org/10.1042/bst20140275

Hook, K. E., Garza, S. J., Lira, M. E., Ching, K. A., Lee, N. V., Cao, J., … Pavlicek, A. (2012). An integrated genomic approach to identify predictive biomarkers of response to the aurora kinase inhibitor PF-03814735. *Molecular Cancer Therapeutics*, *11*(3), 710–719. https://doi.org/10.1158/1535-7163.MCT-11-0184

Huang da, W., Sherman, B. T., & Lempicki, R. A. (2009a). Bioinformatics enrichment tools: Paths toward the comprehensive functional analysis of large gene lists. *Nucleic Acids Research*, *37*(1), 1–13. https://doi.org/10.1093/nar/gkn923

Huang da, W., Sherman, B. T., & Lempicki, R. A. (2009b). Systematic and integrative analysis of large gene lists using DAVID bioinformatics resources. *Nature Protocols*, *4*(1), 44–57. https://doi.org/10.1038/nprot.2008.211

Iness, A. N., Felthousen, J., Ananthapadmanabhan, V., Sesay, F., Saini, S., Guiley, K. Z., … Litovchick, L. (2019). The cell cycle regulatory DREAM complex is disrupted by high expression of oncogenic B-Myb. *Oncogene*, *38*(7), 1080–1092. https://doi.org/10.1038/s41388-018-0490-y

Jin, D., Guo, J., Wu, Y., Du, J., Wang, X., An, J., … Wang, W. (2019). UBE2C, directly targeted by miR-548e-5p, increases the cellular growth and invasive abilities of cancer cells interacting with the EMT marker protein zinc finger E-box binding homeobox 1/2 in NSCLC. *Theranostics*, *9*(7), 2036–2055. https://doi.org/10.7150/thno.32738

Jin, Y., Zhu, H., Cai, W., Fan, X., Wang, Y., Niu, Y., … Bu, Y. (2017). B-Myb is up-regulated and promotes cell growth and motility in non-small cell lung Cancer. *International Journal of Molecular Sciences*, *18*(6), 860. https://doi.org/10.3390/ijms18060860

Kagawa, N., Hori, T., Hoki, Y., Hosoya, O., Tsutsui, K., Saga, Y., … Fukagawa, T. (2014). The CENP-O complex requirement varies among different cell types. *Chromosome Research*, *22*(3), 293–303. https://doi.org/10.1007/s10577-014-9404-1

Karlsson, A., Brunnström, H., Lindquist, K. E., Jirström, K., Jönsson, M., Rosengren, F., … Staaf, J. (2015). Mutational and gene fusion analyses of primary large cell and large cell neuroendocrine lung cancer. *Oncotarget*, *6*(26), 22028–22037. https://doi.org/10.18632/oncotarget.4314

Karlsson, A., Jonsson, M., Lauss, M., Brunnstrom, H., Jonsson, P., Borg, A., … Staaf, J. (2014). Genome-wide DNA methylation analysis of lung carcinoma reveals one neuroendocrine and four adenocarcinoma epitypes associated with patient outcome. *Clinical Cancer Research*, *20*(23), 6127–6140. https://doi.org/10.1158/1078-0432.ccr-14-1087

Kim, H. S., Lee, J. H., Nam, S. J., Ock, C.-Y., Moon, J.-W., Yoo, C. W., … Han, J.-Y. (2018). Association of PD-L1 expression with tumor-infiltrating immune cells and mutation burden in high-grade neuroendocrine carcinoma of the lung. *Journal of Thoracic Oncology*, *13*(5), 636–648. https://doi.org/10.1016/j.jtho.2018.01.008

Kucuksayan, H., Akgun, S., Ozes, O. N., Alikanoglu, A. S., Yildiz, M., Dal, E., & Akca, H. (2019). TGF-beta-SMAD-miR-520e axis regulates NSCLC metastasis through a TGFBR2-mediated negative-feedback loop. *Carcinogenesis*, *40*(5), 695–705. https://doi.org/10.1093/carcin/bgy166

Kujtan, L., Muthukumar, V., Kennedy, K. F., Davis, J. R., Masood, A., & Subramanian, J. (2018). The Role of systemic therapy in the management of stage I large cell neuroendocrine carcinoma of the lung. *Journal of Thoracic Oncology*, *13*(5), 707–714. https://doi.org/10.1016/j.jtho.2018.01.019

Lai, J., Yang, H., Zhu, Y., Ruan, M., Huang, Y., & Zhang, Q. (2019). MiR-7-5p-mediated downregulation of PARP1 impacts DNA homologous recombination repair and resistance to doxorubicin in small cell lung cancer. *BMC Cancer*, *19*(1), 602. https://doi.org/10.1186/s12885-019-5798-7

Lan, J., Huang, H.-Y., Lee, S.-W., Chen, T.-J., Tai, H.-C., Hsu, H.-P., … Li, C.-F. (2014). TOP2A overexpression as a poor prognostic factor in patients with nasopharyngeal carcinoma. *Tumour Biology*, *35*(1), 179–187. https://doi.org/10.1007/s13277-013-1022-6

Li, H., Zhang, H., & Wang, Y. (2018). Centromere protein U facilitates metastasis of ovarian cancer cells by targeting high mobility group box 2 expression. *American Journal of Cancer Research*, *8*(5), 835–851.

Li, J., Wang, Z. G., Pang, L. B., Zhang, R. H., & Wang, Y. Y. (2019). Reduced CENPU expression inhibits lung adenocarcinoma cell proliferation and migration through PI3K/AKT signaling. *Bioscience,*

Biotechnology, and Biochemistry, *83*(6), 1077–1084. https://doi.org/10.1080/09168451.2019.1588094

Li, P., Ma, L., Zhang, Y., Ji, F., & Jin, F. (2014). MicroRNA-137 down-regulates KIT and inhibits small cell lung cancer cell proliferation. *Biomedicine and Pharmacotherapy*, *68*(1), 7–12. https://doi.org/10.1016/j.biopha.2013.12.002

Li, Q., Ran, P., Zhang, X., Guo, X., Yuan, Y., Dong, T., … Xiao, C. (2018). Downregulation of N-Acetylglucosaminyltransferase GCNT3 by miR-302b-3p decreases non-small cell lung cancer (NSCLC) cell proliferation, migration and invasion. *Cellular Physiology and Biochemistry*, *50*(3), 987–1004. https://doi.org/10.1159/000494482

Li, T. K., & Liu, L. F. (2001). Tumor cell death induced by topoisomerase-targeting drugs. *Annual Review of Pharmacology and Toxicology*, *41*, 53–77. https://doi.org/10.1146/annurev.pharmtox.41.1.53

Li, W., & He, F. (2014). Monocyte to macrophage differentiation-associated (MMD) targeted by miR-140-5p regulates tumor growth in non-small cell lung cancer. *Biochemical and Biophysical Research Communications*, *450*(1), 844–850. https://doi.org/10.1016/j.bbrc.2014.06.075

Li, X., Fu, Q., Li, H., Zhu, L., Chen, W., Ruan, T., … Yu, X. (2019). MicroRNA-520c-3p functions as a novel tumor suppressor in lung adenocarcinoma. *FEBS Journal*, *286*(14), 2737–2752. https://doi.org/10.1111/febs.14835

Li, Y., Cui, X., Li, Y., Zhang, T., & Li, S. (2018). Upregulated expression of miR-421 is associated with poor prognosis in non-small-cell lung cancer. *Cancer Management and Research*, *10*, 2627–2633. https://doi.org/10.2147/cmar.s167432

Li, Y., Shen, X., Wang, X., Li, A., Wang, P., Jiang, P., … Feng, Q. (2015). EGCG regulates the cross-talk between JWA and topoisomerase IIalpha in non-small-cell lung cancer (NSCLC) cells. *Scientific Reports*, *5*, 11009. https://doi.org/10.1038/srep11009

Lin, C., Xie, L., Lu, Y., Hu, Z., & Chang, J. (2018). miR-133b reverses cisplatin resistance by targeting GSTP1 in cisplatin-resistant lung cancer cells. *International Journal of Molecular Medicine*, *41*(4), 2050–2058. https://doi.org/10.3892/ijmm.2018.3382

Liu, C. H., Lv, D. S., Li, M., Sun, G., Zhang, X. F., & Bai, Y. (2017). MicroRNA-4458 suppresses the proliferation of human lung cancer cells in vitro by directly targeting Lin28B. *Acta Pharmacologica Sinica*, *38*(9), 1297–1304. https://doi.org/10.1038/aps.2017.73

Liu, G., Li, Y. I., & Gao, X. (2016). Overexpression of microRNA-133b sensitizes non-small cell lung cancer cells to irradiation through the inhibition of glycolysis. *Oncology Letters*, *11*(4), 2903–2908. https://doi.org/10.3892/ol.2016.4316

Liu, J., Liu, S., Deng, X., Rao, J., Huang, K., Xu, G., & Wang, X. (2019). MicroRNA-582-5p suppresses non-small cell lung cancer cells growth and invasion via downregulating NOTCH1. *PLoS ONE*, *14*(6), e0217652. https://doi.org/10.1371/journal.pone.0217652

Liu, L., Liu, L., & Lu, S. (2019). lncRNA H19 promotes viability and epithelial-mesenchymal transition of lung adenocarcinoma cells by targeting miR-29b-3p and modifying STAT3. *International Journal of Oncology*, *54*(3), 929–941. https://doi.org/10.3892/ijo.2019.4695

Liu, W. T., Wang, Y., Zhang, J., Ye, F., Huang, X. H., Li, B., & He, Q. Y. (2018). A novel strategy of integrated microarray analysis identifies CENPA, CDK1 and CDC20 as a cluster of diagnostic biomarkers in lung adenocarcinoma. *Cancer Letters*, *425*, 43–53. https://doi.org/10.1016/j.canlet.2018.03.043

Liu, X., Liu, J., Zhang, X., Tong, Y., & Gan, X. (2019). MiR-520b promotes the progression of non-small cell lung cancer through activating Hedgehog pathway. *Journal of Cellular and Molecular Medicine*, *23*(1), 205–215. https://doi.org/10.1111/jcmm.13909

Liu, Y., Miao, L., Ni, R., Zhang, H., Li, L., Wang, X., … Wang, J. (2016). microRNA-520a-3p inhibits proliferation and cancer stem cell phenotype by targeting HOXD8 in non-small cell lung cancer. *Oncology Reports*, *36*(6), 3529–3535. https://doi.org/10.3892/or.2016.5149

Long, E. M., Long, M. A., Tsirigotis, M., & Gray, D. A. (2003). Stimulation of the murine Uchl1 gene promoter by the B-Myb transcription factor. *Lung Cancer*, *42*(1), 9–21. https://doi.org/10.1016/s0169-5002(03)00279-4

Lu, Y., Liu, Y., Jiang, J., Xi, Z., Zhong, N., Shi, S., … Wei, X. (2014). Knocking down the expression of aurora-A gene inhibits cell proliferation and induces G2/M phase arrest in human small cell lung cancer cells. *Oncology Reports*, *32*(1), 243–249. https://doi.org/10.3892/or.2014.3194

Luo, J., Zhu, H., Jiang, H., Cui, Y., Wang, M., Ni, X., & Ma, C. (2018). The effects of aberrant expression of LncRNA DGCR5/miR-873-5p/TUSC3 in lung cancer cell progression. *Cancer Medicine*, *7*(7), 3331–3341. https://doi.org/10.1002/cam4.1566

Makino, T., Mikami, T., Hata, Y., Otsuka, H., Koezuka, S., Isobe, K., … Iyoda, A. (2016). Comprehensive biomarkers for personalized treatment in pulmonary large cell neuroendocrine carcinoma: A comparative analysis with adenocarcinoma. *Annals of Thoracic Surgery*, *102*(5), 1694–1701. https://doi.org/10.1016/j.athoracsur.2016.04.100

Mao, Y., Xue, P., Li, L., Xu, P., Cai, Y., Chu, X., … Zhu, S. (2019). Bioinformatics analysis of mRNA and miRNA microarray to identify the key miRNAgene pairs in smallcell lung cancer. *Mol Med Rep*, *20*(3), 2199–2208. https://doi.org/10.3892/mmr.2019.10441

Mayer, R. J. (2000). The meteoric rise of regulated intracellular proteolysis. *Nature Reviews Molecular Cell Biology*, *1*(2), 145–148. https://doi.org/10.1038/35040090

Miyoshi, T., Umemura, S., Matsumura, Y., Mimaki, S., Tada, S., Makinoshima, H., … Tsuchihara, K. (2017). Genomic profiling of large-cell neuroendocrine carcinoma of the lung. *Clinical Cancer Research*, *23*(3), 757–765. https://doi.org/10.1158/1078-0432.ccr-16-0355

Mizuno, K., Mataki, H., Arai, T., Okato, A., Kamikawaji, K., Kumamoto, T., … Seki, N. (2017). The microRNA expression signature of small cell lung cancer: Tumor suppressors of miR-27a-5p and miR-34b-3p and their targeted oncogenes. *Journal of Human Genetics*, *62*(7), 671–678. https://doi.org/10.1038/jhg.2017.27

Musa, J., Aynaud, M. M., Mirabeau, O., Delattre, O., & Grunewald, T. G. (2017). MYBL2 (B-Myb): A central regulator of cell proliferation, cell survival and differentiation involved in tumorigenesis. *Cell Death and Disease*, *8*(6), e2895. https://doi.org/10.1038/cddis.2017.244

Nabetani, A., Koujin, T., Tsutsumi, C., Haraguchi, T., & Hiraoka, Y. (2001). A conserved protein, Nuf2, is implicated in connecting the centromere to the spindle during chromosome segregation: A link between the kinetochore function and the spindle checkpoint. *Chromosoma*, *110*(5), 322–334. https://doi.org/10.1007/s00412010153

Nagel, R., Avelar, A. T., Aben, N., Proost, N., van de Ven, M., van der Vliet, J., … Berns, A. (2019). Inhibition of the replication stress response is a synthetic vulnerability in SCLC that acts synergistically in combination with cisplatin. *Molecular Cancer Therapeutics*, *18*(4), 762–770. https://doi.org/10.1158/1535-7163.mct-18-0972

Neubauer, E., Wirtz, R. M., Kaemmerer, D., Athelogou, M., Schmidt, L., Sanger, J., & Lupp, A. (2016). Comparative evaluation of three

proliferation markers, Ki-67, TOP2A, and RacGAP1, in bronchopulmonary neuroendocrine neoplasms: Issues and prospects. *Oncotarget*, *7*(27), 41959–41973. https://doi.org/10.18632/oncotarget.9747

Olaussen, K. A., & Postel-Vinay, S. (2016). Predictors of chemotherapy efficacy in non-small-cell lung cancer: A challenging landscape. *Annals of Oncology*, *27*(11), 2004–2016. https://doi.org/10.1093/annonc/mdw321

Pan, X., Chen, Y., Shen, Y., & Tantai, J. (2019). Knockdown of TRIM65 inhibits autophagy and cisplatin resistance in A549/DDP cells by regulating miR-138-5p/ATG7. *Cell Death and Disease*, *10*(6), 429. https://doi.org/10.1038/s41419-019-1660-8

Pathan, M., Keerthikumar, S., Chisanga, D., Alessandro, R., Ang, C.-S., Askenase, P., … Mathivanan, S. (2017). A novel community driven software for functional enrichment analysis of extracellular vesicles data. *Journal of Extracellular Vesicles*, *6*(1), 1321455. https://doi.org/10.1080/20013078.2017.1321455

Psyrri, A., Kalogeras, K. T., Kronenwett, R., Wirtz, R. M., Batistatou, A., Bournakis, E., … Fountzilas, G. (2012). Prognostic significance of UBE2C mRNA expression in high-risk early breast cancer. A Hellenic Cooperative Oncology Group (HeCOG) Study. *Annals of Oncology*, *23*(6), 1422–1427. https://doi.org/10.1093/annonc/mdr527

Rekhtman, N., Pietanza, M. C., Hellmann, M. D., Naidoo, J., Arora, A., Won, H., … Ladanyi, M. (2016). Next-generation sequencing of pulmonary large cell neuroendocrine carcinoma reveals small cell carcinoma-like and non-small cell carcinoma-like subsets. *Clinical Cancer Research*, *22*(14), 3618–3629. https://doi.org/10.1158/1078-0432.ccr-15-2946

Rossi, G., Cavazza, A., Marchioni, A., Longo, L., Migaldi, M., Sartori, G., … Brambilla, E. (2005). Role of chemotherapy and the receptor tyrosine kinases KIT, PDGFRalpha, PDGFRbeta, and Met in large-cell neuroendocrine carcinoma of the lung. *Journal of Clinical Oncology*, *23*(34), 8774–8785. https://doi.org/10.1200/jco.2005.02.8233

Rupaimoole, R., & Slack, F. J. (2017). MicroRNA therapeutics: Towards a new era for the management of cancer and other diseases. *Nature Reviews Drug Discovery*, *16*(3), 203–222. https://doi.org/10.1038/nrd.2016.246

Saunders, L. R., Bankovich, A. J., Anderson, W. C., Aujay, M. A., Bheddah, S., Black, K. A., … Dylla, S. J. (2015). A DLL3-targeted antibody-drug conjugate eradicates high-grade pulmonary neuroendocrine tumor-initiating cells in vivo. *Science Translational Medicine*, *7*(302), 302ra136. https://doi.org/10.1126/scitranslmed.aac9459

Shah, K. N., Bhatt, R., Rotow, J., Rohrberg, J., Olivas, V., Wang, V. E., … Bandyopadhyay, S. (2019). Aurora kinase A drives the evolution of resistance to third-generation EGFR inhibitors in lung cancer. *Nature Medicine*, *25*(1), 111–118. https://doi.org/10.1038/s41591-018-0264-7

Shannon, P., Markiel, A., Ozier, O., Baliga, N. S., Wang, J. T., Ramage, D., … Ideker, T. (2003). Cytoscape: A software environment for integrated models of biomolecular interaction networks. *Genome Research*, *13*(11), 2498–2504. https://doi.org/10.1101/gr.1239303

Sim, J., Kim, Y., Kim, H., Shin, S. J., Kim, D. H., Paik, S. S., & Jang, K. (2018). Identification of recurrence-associated microRNAs in stage I lung adenocarcinoma. *Medicine (Baltimore)*, *97*(25), e10996. https://doi.org/10.1097/md.0000000000010996

Simbolo, M., Mafficini, A., Sikora, K. O., Fassan, M., Barbi, S., Corbo, V., … Scarpa, A. (2017). Lung neuroendocrine tumours: Deep sequencing of the four World Health Organization histotypes reveals chromatin-remodelling genes as major players and a prognostic role for TERT, RB1, MEN1 and KMT2D. *The Journal of Pathology*, *241*(4), 488–500. https://doi.org/10.1002/path.4853

Sivakumar, S., Lucas, F. A. S., McDowell, T. L., Lang, W., Xu, L. I., Fujimoto, J., … Kadara, H. (2017). Genomic landscape of atypical adenomatous hyperplasia reveals divergent modes to lung adenocarcinoma. *Cancer Research*, *77*(22), 6119–6130. https://doi.org/10.1158/0008-5472.can-17-1605

Soues, S., Wiltshire, M., & Smith, P. J. (2001). Differential sensitivity to etoposide (VP-16)-induced S phase delay in a panel of small-cell lung carcinoma cell lines with G1/S phase checkpoint dysfunction. *Cancer Chemotherapy and Pharmacology*, *47*(2), 133–140. https://doi.org/10.1007/s002800000227

Su, T. J., Ku, W. H., Chen, H. Y., Hsu, Y. C., Hong, Q. S., Chang, G. C., … Chen, J. J. (2016). Oncogenic miR-137 contributes to cisplatin resistance via repressing CASP3 in lung adenocarcinoma. *American Journal of Cancer Research*, *6*(6), 1317–1330.

Szklarczyk, D., Franceschini, A., Wyder, S., Forslund, K., Heller, D., Huerta-Cepas, J., … von Mering, C. (2015). STRING v10: Protein-protein interaction networks, integrated over the tree of life. *Nucleic Acids Research*, *43*(D1), D447–D452. https://doi.org/10.1093/nar/gku1003

Takada, M., Zhang, W., Suzuki, A., Kuroda, T. S., Yu, Z., Inuzuka, H., … Zhang, Q. (2017). FBW7 loss promotes chromosomal instability and tumorigenesis via cyclin E1/CDK2-mediated phosphorylation of CENP-A. *Cancer Research*, *77*(18), 4881–4893. https://doi.org/10.1158/0008-5472.can-17-1240

Tang, L. X., Chen, G. H., Li, H., He, P., Zhang, Y., & Xu, X. W. (2018). Long non-coding RNA OGFRP1 regulates LYPD3 expression by sponging miR-124-3p and promotes non-small cell lung cancer progression. *Biochemical and Biophysical Research Communications*, *505*(2), 578–585. https://doi.org/10.1016/j.bbrc.2018.09.146

Travis, W. D., Brambilla, E., Burke, A. P., Marx, A., & Nicholson, A. G. (2015). Introduction to The 2015 World Health Organization Classification of tumors of the lung, pleura, thymus, and heart. *Journal of Thoracic Oncology*, *10*(9), 1240–1242. https://doi.org/10.1097/jto.0000000000000663

Tzelepi, V., Zhang, J., Lu, J.-F., Kleb, B., Wu, G., Wan, X., … Aparicio, A. M. (2012). Modeling a lethal prostate cancer variant with small-cell carcinoma features. *Clinical Cancer Research*, *18*(3), 666–677. https://doi.org/10.1158/1078-0432.CCR-11-1867

Vader, G., & Lens, S. M. (2008). The Aurora kinase family in cell division and cancer. *Biochimica et Biophysica Acta*, *1786*(1), 60–72. https://doi.org/10.1016/j.bbcan.2008.07.003

van Ree, J. H., Jeganathan, K. B., Malureanu, L., & van Deursen, J. M. (2010). Overexpression of the E2 ubiquitin-conjugating enzyme UbcH10 causes chromosome missegregation and tumor formation. *Journal of Cell Biology*, *188*(1), 83–100. https://doi.org/10.1083/jcb.200906147

Vlotides, G., Eigler, T., & Melmed, S. (2007). Pituitary tumor-transforming gene: Physiology and implications for tumorigenesis. *Endocrine Reviews*, *28*(2), 165–186. https://doi.org/10.1210/er.2006-0042

Vogelstein, B., Papadopoulos, N., Velculescu, V. E., Zhou, S., Diaz, L. A. Jr, & Kinzler, K. W. (2013). Cancer genome landscapes. *Science*, *339*(6127), 1546–1558. https://doi.org/10.1126/science.1235122

Walker, M. G. (2001). Drug target discovery by gene expression analysis: Cell cycle genes. *Current Cancer Drug Targets*, *1*(1), 73–83.

Walter, R. B., Walter, D. J., Boswell, W. T., Caballero, K. L., Boswell, M., Lu, Y., … Savage, M. G. (2015). Exposure to fluorescent light

triggers down regulation of genes involved with mitotic progression in Xiphophorus skin. *Comparative Biochemistry and Physiology Part C: Toxicology and Pharmacology*, *178*, 93–103. https://doi.org/10.1016/j.cbpc.2015.08.006

Wang, F., Liu, Y., & Chen, Y. (2016). Pituitary tumor transforming gene-1 in non-small cell lung cancer: Clinicopathological and immunohistochemical analysis. *Biomedicine and Pharmacotherapy*, *84*, 1595–1600. https://doi.org/10.1016/j.biopha.2016.10.047

Wang, S., Liu, B., Zhang, J., Sun, W., Dai, C., Sun, W., & Li, Q. (2017). Centromere protein U is a potential target for gene therapy of human bladder cancer. *Oncology Reports*, *38*(2), 735–744. https://doi.org/10.3892/or.2017.5769

Wang, W., Cao, R., Su, W., Li, Y., & Yan, H. (2019). miR-655-3p inhibits cell migration and invasion by targeting pituitary tumor-transforming 1 in non-small cell lung cancer. *Bioscience, Biotechnology, and Biochemistry*, *1–6*, https://doi.org/10.1080/09168451.2019.1617109

Wang, X., Chen, D., Gao, J., Long, H., Zha, H., Zhang, A., … Wu, W. (2018). Centromere protein U expression promotes non-small-cell lung cancer cell proliferation through FOXM1 and predicts poor survival. *Cancer Management and Research*, *10*, 6971–6984. https://doi.org/10.2147/cmar.s182852

Wang, X.-C., Yue, X., Zhang, R.-X., Liu, T.-Y., Pan, Z.-Z., Yang, M.-J., … Liu, R.-Y. (2019). Genome-wide RNAi screening identifies RFC4 as a factor that mediates radioresistance in colorectal cancer by facilitating nonhomologous end joining repair. *Clinical Cancer Research*, *25*(14), 4567–4579. https://doi.org/10.1158/1078-0432.ccr-18-3735

Wei, T., Weiler, S. M. E., Tóth, M., Sticht, C., Lutz, T., Thomann, S., … Breuhahn, K. (2019). YAP-dependent induction of UHMK1 supports nuclear enrichment of the oncogene MYBL2 and proliferation in liver cancer cells. *Oncogene*, *38*(27), 5541–5550. https://doi.org/10.1038/s41388-019-0801-y

Wesierska-Gadek, J., & Skladanowski, A. (2012). Therapeutic intervention by the simultaneous inhibition of DNA repair and type I or type II DNA topoisomerases: One strategy, many outcomes. *Future Med Chem*, *4*(1), 51–72. https://doi.org/10.4155/fmc.11.175

Wu, A., Li, J., Wu, K., Mo, Y., Luo, Y., Ye, H., … Yang, Z. (2015). MiR-373-3p promotes invasion and metastasis of lung adenocarcinoma cells. *Zhongguo Fei Ai Za Zhi*, *18*(7), 427–435. https://doi.org/10.3779/j.issn.1009-3419.2015.07.07

Wu, F., Mo, Q., Wan, X., Dan, J., & Hu, H. (2019). NEAT1/hsa-mir-98-5p/MAPK6 axis is involved in non-small-cell lung cancer development. *Journal of Cellular Biochemistry*, *120*(3), 2836–2846. https://doi.org/10.1002/jcb.26442

Wu, Q., Chen, Y.-F., Fu, J., You, Q.-H., Wang, S.-M., Huang, X., … Zhang, S.-H. (2014). Short hairpin RNA-mediated down-regulation of CENP-A attenuates the aggressive phenotype of lung adenocarcinoma cells. *Cellular Oncology (Dordr)*, *37*(6), 399–407. https://doi.org/10.1007/s13402-014-0199-z

Wu, Q., Qian, Y. M., Zhao, X. L., Wang, S. M., Feng, X. J., Chen, X. F., & Zhang, S. H. (2012). Expression and prognostic significance of centromere protein A in human lung adenocarcinoma. *Lung Cancer*, *77*(2), 407–414. https://doi.org/10.1016/j.lungcan.2012.04.007

Wu, Q., Zhang, B., Sun, Y., Xu, R., Hu, X., Ren, S., … Wang, Z. (2019). Identification of novel biomarkers and candidate small molecule drugs in non-small-cell lung cancer by integrated microarray analysis. *OncoTargets and Therapy*, *12*, 3545–3563. https://doi.org/10.2147/ott.s198621

Xia, H., Jing, H., Li, Y., & Lv, X. (2018). Long noncoding RNA HOXD-AS1 promotes non-small cell lung cancer migration and invasion through regulating miR-133b/MMP9 axis. *Biomedicine and Pharmacotherapy*, *106*, 156–162. https://doi.org/10.1016/j.biopha.2018.06.073

Xiang, J., Fang, L., Luo, Y., Yang, Z., Liao, Y. I., Cui, J. I., … Wang, J. (2014). Levels of human replication factor C4, a clamp loader, correlate with tumor progression and predict the prognosis for colorectal cancer. *Journal of Translational Medicine*, *12*, 320. https://doi.org/10.1186/s12967-014-0320-0

Xu, F., Chen, K. E., Lu, C., Gu, J., Zeng, H., Xu, Y., … Ge, D. I. (2019). Large cell neuroendocrine carcinoma shares similarity with small cell carcinoma on the basis of clinical and pathological features. *Translational Oncology*, *12*(4), 646–655. https://doi.org/10.1016/j.tranon.2019.01.004

Xu, G., Cai, J., Wang, L., Jiang, L., Huang, J., Hu, R., & Ding, F. (2018). MicroRNA-30e-5p suppresses non-small cell lung cancer tumorigenesis by regulating USP22-mediated Sirt1/JAK/STAT3 signaling. *Experimental Cell Research*, *362*(2), 268–278. https://doi.org/10.1016/j.yexcr.2017.11.027

Xu, X., Jin, S., Ma, Y., Fan, Z., Yan, Z., Li, W., … Ye, Q. (2017). miR-30a-5p enhances paclitaxel sensitivity in non-small cell lung cancer through targeting BCL-2 expression. *Journal of Molecular Medicine (Berlin)*, *95*(8), 861–871. https://doi.org/10.1007/s00109-017-1539-z

Yuan, W., Xie, S., Wang, M., Pan, S., Huang, X., Xiong, M., … Shao, L. (2018). Bioinformatic analysis of prognostic value of ZW10 interacting protein in lung cancer. *OncoTargets and Therapy*, *11*, 1683–1695. https://doi.org/10.2147/ott.s149012

Zeng, Z., Li, Y., Pan, Y., Lan, X., Song, F., Sun, J., … Liang, L. I. (2018). Cancer-derived exosomal miR-25-3p promotes pre-metastatic niche formation by inducing vascular permeability and angiogenesis. *Nature Communications*, *9*(1), 5395. https://doi.org/10.1038/s41467-018-07810-w

Zhang, L., Hao, C., Zhai, R., Wang, D. I., Zhang, J., Bao, L., … Yao, W. U. (2018). Downregulation of exosomal let-7a-5p in dust exposed- workers contributes to lung cancer development. *Respiratory Research*, *19*(1), 235. https://doi.org/10.1186/s12931-018-0949-y

Zhang, L., Ji, G., Shao, Y., Qiao, S., Jing, Y., Qin, R., … Shao, C. (2015). MLF1 interacting protein: A potential gene therapy target for human prostate cancer? *Medical Oncology*, *32*(2), 454. https://doi.org/10.1007/s12032-014-0454-1

Zhang, L., Qian, J., Qiang, Y., Huang, H., Wang, C., Li, D., & Xu, B. (2014). Down-regulation of miR-4500 promoted non-small cell lung cancer growth. *Cellular Physiology and Biochemistry*, *34*(4), 1166–1174. https://doi.org/10.1159/000366329

Zhang, Q., Li, Y. D., Zhang, S. X., & Shi, Y. Y. (2018). Centromere protein U promotes cell proliferation, migration and invasion involving Wnt/beta-catenin signaling pathway in non-small cell lung cancer. *European Review for Medical and Pharmacological Sciences*, *22*(22), 7768–7777. https://doi.org/10.26355/eurrev_201811_16400

Zhang, X., He, X., Liu, Y., Zhang, H., Chen, H., Guo, S., & Liang, Y. (2017). MiR-101-3p inhibits the growth and metastasis of non-small cell lung cancer through blocking PI3K/AKT signal pathway by targeting MALAT-1. *Biomedicine and Pharmacotherapy*, *93*, 1065–1073. https://doi.org/10.1016/j.biopha.2017.07.005

Zhou, D. H., Wang, X., & Feng, Q. (2014). EGCG enhances the efficacy of cisplatin by downregulating hsa-miR-98-5p in NSCLC A549 cells. *Nutrition and Cancer*, *66*(4), 636–644. https://doi.org/10.1080/01635581.2014.894101

Zhu, J., Zeng, Y., Li, W., Qin, H., Lei, Z., Shen, D., … Liu, Z. (2017). CD73/NT5E is a target of miR-30a-5p and plays an important role in the pathogenesis of non-small cell lung cancer. *Molecular Cancer*, *16*(1), 34. https://doi.org/10.1186/s12943-017-0591-1

How to cite this article: Dong S, Liang J, Zhai W, Yu Z. Common and distinct features of potentially predictive biomarkers in small cell lung carcinoma and large cell neuroendocrine carcinoma of the lung by systematic and integrated analysis. *Mol Genet Genomic Med*. 2020;8:e1126. https://doi.org/10.1002/mgg3.1126